

THE EFFECTS OF TEMPERATURE AND GAMMA RAY  
RADIATION ON CURRENT SATURATION  
IN CADMIUM SULFIDE FILMS

---

A THESIS SUBMITTED IN PARTIAL FULFILLMENT OF THE  
REQUIREMENTS FOR THE DEGREE OF

MASTER OF SCIENCE

IN THE DEPARTMENT OF ELECTRICAL ENGINEERING  
UNIVERSITY OF MANITOBA

BY

AVINASH SADHU

OCT. 1970



### ACKNOWLEDGMENT

The author wishes to thank Dr. K.C. Kao for his unfailing guidance and encouragement throughout the work on this thesis. The technical assistance given by the offices of Mr. R. Wood and Mr. John Elliot is sincerely appreciated.

The author is also indebted to the University of Manitoba for the reward of a fellowship and the National Research Council and Defence Research Board of Canada for the grants made to Dr. K. C. Kao by which this research was partially supported.

Special thanks are due to Miss Jo-Anne Abrams for typing this thesis.

## ABSTRACT

The effect of temperature on the photocurrent in CdS films has been used as a tool to establish that the current saturation observed at high field is due to acoustoelectric effect. The films were prepared by vacuum evaporation and subsequently heat-treated in order to compensate for the native astoichiometicities.

The effect of radiation has also been studied. Results show that the saturation current decreases with increasing doses of radiation.

LIST OF FIGURES

III

- Fig. 1 A phenomenological model for the interpretation of acoustoelectric effect as developed by Rose (1966).
- Fig. 2 Experimental arrangement used by McFee et al (1966).
- Fig. 3 A simplified model of electron-phonon interaction.
- Fig. 4 The distribution of electric field as a function of distance (Haydl, 1967).
- Fig. 5 Energy level diagram with a single trap level.
- Fig. 6 Model of an inhomogeneous sample.
- Fig. 7 Method of heat-treatment of CdS films.
- Fig. 8 X-ray diffraction pattern to determine the orientation of the films.
- Fig. 9 Measurement of the thickness of the film using an interferometer.
- Fig. 10 Sample geometry.
- Fig. 11 Circuit used for the measurement of the V-I characteristics of the film.
- Fig. 12 Sample holder.
- Fig. 13 The effect of illumination on the threshold field for current saturation.
- Fig. 14 The effect of temperature on the saturation current.
- Fig. 15 The behaviour of photocurrent for fields above the threshold field for current saturation.
- Fig. 16 The effect of temperature on the threshold field for current saturation.

Fig. 17 The effect of gamma-ray radiation on current saturation.

Fig. 18 The dark and light resistivities as a function of  $1/T$

Fig. 19 A photomicrograph of a vacuum deposited CdS film at a magnification of  $10^3$ .

Fig. 20 Circuit diagram of the pulse generator.

Fig. 21 A&B Oscilloscope photographs of the output pulses of the pulse generator.

TABLE OF CONTENTS

ACKNOWLEDGMENT	I
ABSTRACT	II
TABLE OF FIGURES	III
Chapter 1. INTRODUCTION	1
Chapter 2. REVIEW OF PREVIOUS WORK RELATED TO THE SUBJECT	5
2.1 Preparation of CdS films.	5
2.2 Defects in CdS films	7
2.3 Acoustoelectric effects	9
2.3.1 Experimental work	9
2.3.2 Theory	12
2.4 The effect of traps	19
2.5 The effect of non-homogeneity	25
Chapter 3. FABRICATION OF CdS FILMS AND EXPERIMENTAL TECHNIQUES	29
3.1 Fabrication technique	30
3.2. Post-evaporation heat-treatment	31
3.2.1 Method of heat-treatment	32
3.2.2 Effect of heat-treatment	36
3.3 Ohmic contacts	37

Chapter 4 EXPERIMENTAL RESULTS AND DISCUSSION	38
4.1 The effect of temperature, illumination and gamma ray radiation	38
4.2 Discussion	43
Chapter 5 CONCLUSION	53
BIBLIOGRAPHY	54
Appendix. DESIGN OF PULSE GENERATOR	61

## CHAPTER 1

## INTRODUCTION

Cadmium Sulphide is one of the most important compound semiconductors. It has been studied extensively and has been considered as a special material for advancing the understanding of the physics and chemistry of wide band-gap solids. This material exhibits many interesting electro-optical phenomena on which many electronic devices such as field-effect transistors, image intensifiers and storage devices are based.

In 1957 Paramenter predicted the existence of the acoustoelectric effect in piezoelectric semiconductors, and in 1958 Krömer proposed that the negative differential conductivity in solids at high field can be used for amplification in practical devices. In 1960 Nine reported the observation of longitudinal and shear ultrasonic waves travelling respectively parallel to and normal to the hexagonal axis of single crystals of CdS, but he failed to consider piezoelectric interactions as a possible mechanism for his observation. Shortly afterwards, Hutson (1960) measured the electro-mechanical coupling constants of both CdS and ZnO and realized that coupling between phonons and electrons could cause the

type of acoustic attenuation and dispersion observed by Nine (1960). Two fundamentally important phenomena emerged from the study undertaken by Hutson (1961), of the photo-sensitive ultrasonic attenuation in CdS as a function of applied electric field. The first confirmed the earlier prediction of White (1962) that when the velocity of electrons exceeded the velocity of sound, the sign of acoustic attenuation reversed. The second showed that there was no need for an input R. F. signal which was previously thought to be necessary to produce sufficient acoustic noise input signal for amplification. The thermal noise generated in the crystal is sufficient to build the acoustic flux up to a level required to cause current saturation or oscillations in it. These researches culminated in the observations of "high field domains" which formed near an electrode and travelled through the sample at a velocity of the order of  $10^5$  cm/sec. (Haydl et al. 1965).

The interest in the study of thin films has grown considerably after the introduction of integrated circuits. Butler and Sandbank (1967) have discussed the possibility of using the travelling domains for integrated circuits. It is possible to produce a circuit using only one bulk effect which would normally require a large assembly of active and passive components. The domains generated in a piezoelectric material due to acoustoelectric effect travel at the velocity

of sound ( $5 \times 10^5$  cm/sec.), while those produced due to other effects such as the Gunn effect travel at about  $10^7$  cm/sec. The former is more useful than the latter because the latter produces an embarrassingly high bit rate for use in digital mode systems. Moreover, the domain formation in piezoelectric semiconductors such as CdS and ZnO can be controlled by means of visible light while for the high velocity domains infra-red light has to be used which may limit their application. There are also many potential applications of piezoelectric effects in semiconductors such as optical scanning, visual display, synthesis of complex electronic functions by geometric or electronic field profile shaping, and transducers, etc.

Thin films can be deposited either on conducting metal substrates or on dielectric substrates. For the former, the substrate may act as heat sink for the thin film circuits operated at lower power levels as compared to their bulk counterparts. Thus thin film acoustoelectric devices have certain advantages over the crystals for mass production, low production cost and microelectronics.

CdS films were chosen for the present investigation because of their unique properties of piezoelectricity and photoconductivity, and the easiness in obtaining the material of high purity and in fabricating epitaxial layers.

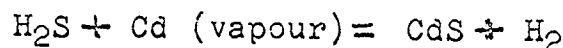
The current saturation in crystals has been attributed to two possible mechanisms, namely field enhanced

trapping and acoustoelectric effect. In the present investigation, we study this phenomenon at various temperatures and illuminations in the hope that the mechanisms responsible for current saturation in CdS films can be identified. The effects of gamma-ray radiation and thermal annealing have also been investigated.

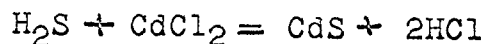
## CHAPTER 2

### REVIEW OF PREVIOUS WORK RELATED TO THE SUBJECT

The potential use of CdS films in photocells was recognized quite early in 1940. The first known method employed by Jacob and Hart (1955) for making photocells is based on an epitaxial vapour carrying process in accordance with the following formula:



A similar process has been adopted recently for producing epitaxial thin films of CdS. which follows



Major research efforts on CdS date back from 1946 when Frerich (1946) worked on the preparation and properties of high-purity, single crystal CdS films. Lorens (1962) extended the work to produce crystals of sufficient perfection by vapour synthesis technique. Inspite of its potential to be useful in industry, the thin film preparation technique is still in its infancy. It is well known that the defect centers and secondary phase effects, play a very important role in the conduction process. The density of such defects varies from sample to sample, and this causes the discrepancy of experimental results.

#### 2.1 PREPARATION OF CdS FILMS

There are a number of techniques for fabricating CdS films which are discussed below along with their advan-

tages and disadvantages. Dresner and Shallcross (1962) analyzed films deposited by vacuum evaporation on glass substrates at  $170^{\circ}\text{C}$  under a residual gas pressure of approximately  $10^{-5}$  Torr. The films were found to be poorly oriented and nonstoichiometric with mobilities of the order of  $1-5 \text{ cm}^2/\text{v-sec}$ . As cadmium and sulphur have different vapour pressures, the use of cadmium sulphide powder alone as a source material results in an undesirable vapour pressure ratio, and hence prevents the deposition of films of good stoichiometry. This difficulty can be overcome either by simultaneously vaporizing CdS and S, or by simultaneously vaporizing Cd and S from separate crucibles. The latter method gives reproducible results. It is an interesting fact that sulphur deposits on substrates at temperatures less than  $50^{\circ}\text{C}$  while cadmium would deposit only at temperatures greater than  $200^{\circ}\text{C}$ . At temperatures between  $50^{\circ}\text{C}$  and  $200^{\circ}\text{C}$  neither cadmium nor sulphur alone would deposit from the vapour unless the other is present to combine to form CdS on the substrate surface. DeKlerk and Kelly (1964) deposited films using two separate baffled sources of cadmium and sulphur and found that the deposited films were highly oriented and stoichiometric. Pizzarello (1964) also deposited films by the method of co-evaporation and confirmed the results of DeKlerk and Kelly. Hudock (1967) deposited CdS film under residual gas pressures of the order of  $10^{-10}$  Torr and found them to be stoichiometric when the substrate temperature was  $450^{\circ}\text{C}$  and

the source temperature was  $470^{\circ}\text{C}$ . Ultrahigh vacuum ( $10^{-10}$  Torr) is essential to get films of considerably high mobility ( $50 \text{ cm}^2/\text{v-sec}$ ). Foster (1966) deposited CdS films using the technique of the co-evaporation of CdS and S<sub>2</sub> on substrates heated at  $180^{\circ}\text{C}$  -  $190^{\circ}\text{C}$ , and the films produced by this method were c-axis oriented and of high resistivity which could be used in transducers without any further treatment.

## 2.2 DEFECTS IN CdS FILMS

It is well known that almost all elements are soluble to a certain extent in CdS. At ordinary temperatures, CdS reacts with the firing environment, and the Gibb's phase diagram shows a small region of existence of compound CdS.

These dissolved elements act as foreign point defects in the film in addition to the native point defects and other thermodynamically unstable defects such as dislocations, internal surfaces and grain boundaries, etc. Even in the absence of foreign defects, the properties of CdS are sensitive to thermal history and the partial pressure of the firing environment. When an undoped CdS crystal is exposed to Cd vapour at high temperatures, excess Cd is incorporated into it interstitially (Boyn 1965). These effects can be considerably reduced by post-evaporation heat treatments (Thermodynamic stabilization). Albers (1967) has classified

them into Cd, S (interstitial),  $V_S$ ,  $V_{Cd}$  (vacancies), and  $Cd_S$ ,  $S_{Cd}$  (substitutional). The first of each of these pairs acts as a donor and the other as an acceptor. Because of their influence on the electronic conductivity of CdS films, these defects have to be eliminated or minimized by heat-treatment.

Amongst the foreign defects the impurities  $H_2O$ , O, Cl, In, Ag, Cu and Au are of particular importance. Cu, Ag and Au diffuse extremely rapidly as interstitials in CdS but they can also substitute for Cd. The presence of donors (such as excess Cd in CdS films) enhances the solubility of Cu and keeps Cu in solution at low temperatures. Cu and Ag act as acceptors electronically. They also precipitate readily to cause imperfections and lattice disorder. In and Ga locate substitutionally at Cd sites, they diffuse rapidly and are highly soluble. Both act as donors and this is the reason why these materials are used for making ohmic contacts on n-type CdS films.

Oxygen would produce a shift in the band gap and energy level of defects (Woodbury 1967). Chemisorbed oxygen acts as an acceptor (Woodbury 1967). Cl acts as a co-activator with Cu in the heat-treatment of CdS films. It may substitute for S and is thought to associate with Cd vacancies during firing (Woodbury 1967). It is well known that water vapour, even a small amount in vacuum deposition chamber, may produce harmful effects on films. Faeth (1967) has suggested

that the presence of  $(H_2O)^-$  ion is responsible for the coulomb repulsive traps located between 0.73ev and 0.83ev below the conduction band of CdS.

### 2.3 ACOUSTOELECTRIC EFFECTS

#### 2.3.1 EXPERIMENTAL WORK

With a CdS crystal sandwiched between two transducers and a d.c. drift field applied across the sample Fig.2 Hutson, McFee and White (1961) observed substantial amplification of ultrasonic waves in photoconductive CdS in the presence of an input R.F. signal. Based on this phenomenon, White (1962) predicted that if the applied d.c. field is sufficient to cause the charge carriers to drift in the direction of ultrasonic wave propagation faster than the velocity of sound, these carriers will react with the sound wave in such a way that the sound wave will be amplified. Another striking observation was the amplification of the ultrasonic wave even in the absence of an input signal (White 1962).

Smith (1962) observed current saturation in CdS crystals. There are several explanations of this phenomenon. Rose (1966) has proposed that when the drift velocity of electrons exceeds the velocity of sound a hypersonic wave is generated, and when the amplitude of the wave is large the electrons will be bunched resulting in potential domains. An increase of the electric field at this point would cause the electrons to be pushed against the walls of the potential wells and would not increase the effective drift field, thus causing saturation. They, however,

failed to detect the presence of hypersonic waves or electromagnetic radiation from bunched electrons.

Hutson (1962) proposed that the current saturation should be regarded as due to the transfer of energy from the drifting electrons to the acoustic waves when their velocity exceeds the velocity of sound. Wang (1962) confirmed this hypothesis by an experiment similar to that of Hutson, McFee and White (1961). Using the same experimental set-up as used by Hutson et al (1961), McFee (1963) observed that in the absence of an input signal, the application of a drift voltage in the direction of the wave propagation changes the attenuation of the ultrasonic wave in CdS and ZnO crystals. This experiment shows that the flux build-up occurs over many round trips of the sound wave in the crystal. It is also shown that the drift current increases abruptly to an initial maximum and then decays to a steady state value which has a striking similarity to the acoustic flux which builds up till it reaches the steady state. Shortening the pulse duration returns the I-V curve to its ohmic behaviour. This verifies that before the ultrasonic flux has time to build up, the current follows the ohm's law.

In a current saturation condition, the entire crystal can be regarded as a resonant cavity supporting coherent standing waves. The oscillations observed during the decay of current from its ohmic value to its saturated value can be attributed to such a coherent acoustic wave

system (McFee 1963).

Okada (1963) on the other hand, observed continuous oscillations by non-uniformly illuminating the crystal. The flux build-up is amplified linearly in the highly illuminated region and it reduces the drift current by non-linear loss mechanism in the low conductivity region. The build-up of flux in the high conductivity region is damped out in the low conductivity region where the amplification of random acoustic flux is not enough to make up for the loss in the opposite direction.

A great deal of experimental work on continuous current oscillation has been published in the past ten years. In 1963 Kikuchi has reported that continuous current oscillations require the light to be shined only on one single spot on the specimen, which corresponds to the photoresponse maximum of the specimen. Reversing the polarity of the bias voltage changes the continuous oscillations to slowly decaying oscillations. The oscillation appears sinusoidal in nature and their period depends on the distance between the electrodes.

Stanley (1967) observed sustained current oscillations in cadmium sulphide crystals in a limited range of voltages. The crystal used was found to be non-uniformly conductive.

Yee et al (1969) reported that the acoustoelectric saturation current in CdSe crystals decreases with decreasing temperatures, while Mason (1968) observed that the saturation current decreases with decreasing illumination in CdS thin films.

### 2.3.2 THEORY

To interpret the phenomenon of acoustoelectric interaction, it is convenient to use the phenomenological model developed by Rose (1966) as shown in Fig. 1. In these figures  $V_d$  represents the drift velocity of electrons relative to the static lattice;  $V_s$ , the velocity of sound;  $F_1$ , the force of interaction of electrons with the lattice;  $F_2$ , the frictional force between electrons and active phonons; and  $F_3$ , the force representing phonon-phonon scattering. To simplify the model, let us neglect the forces  $F_1$  and  $F_3$ . Considering that electrons are drifting at a constant velocity  $V_d$ , the system reduces to a system in which only electrons and phonons move parallel to each other as shown in Fig. 3. The power utilized in moving the electrons at a velocity  $V_d$  is

$$P_e = F_2 V_d \quad (2.1)$$

and the power utilized in moving the phonons at a velocity  $V_s$  is

$$P_p = F_2 V_s \quad (2.2)$$

Since the electrons are not accelerated, the power given to the electron stream must be passed on to increasing the momentum of phonons and since all the power given to electrons cannot go into increasing the momentum of phonons, the difference in power

$$P_D = P_e - P_p \quad (2.3)$$

must be dissipated by the system.

Consider an acoustic wave having associated with it an electric field which changes sinusoidally in space and time as does the sound wave. If an acoustic wave is incident to a material in which free carriers drift with the same velocity as the sound wave, there will be no exchange of energy between the electrons and phonons (except the  $I^2R$  loss) because there is no relative motion of electrons and phonons, i.e.  $F_2 = 0$ . In this case, the electrons bunched in the positive troughs of the wave will move with the phase velocity of the wave. But if the drift velocity of electrons is increased by the applied field above the phase velocity of the sound wave, the free electrons will see an alternating electric field due to the sound wave, and this alternating field will increase the dissipative power above that necessary to keep the drift velocity of electrons greater than the phase velocity of the sound wave. Thus the applied field,  $E$ , will consist of two parts:

$$E = \frac{V_d}{\mu} + \frac{F_2}{\rho} \quad (2.4)$$

where  $\frac{F_2}{\rho}$  is the acoustoelectric field generally denoted by Eq.  $\mu$  is the mobility of electrons; and  $\rho$  is the resistivity of the material. Eqn. (2.4) can be written as

$$E = \frac{V_d}{\mu} + E_a \quad (2.5)$$

the current through the sample in the presence of an acoustoelectric field is therefore given by:

$$J = \sigma (E - E_a) \quad (2.6)$$

where  $\sigma$  is the conductivity of the sample. Differentiation of Eqn. (2.6) gives:

$$\frac{dJ}{dE} = \sigma \left(1 - \frac{dE_a}{dE}\right) \quad (2.7)$$

It can be seen that  $\frac{dJ}{dE}$  becomes negative when  $\frac{dE_a}{dE} > 1$ .

Therefore the minimum threshold field for a negative differential conductivity will be given by:

$$\frac{dE_a}{dE} = 1 \quad (2.8)$$

Since the acoustoelectric field depends on the magnitude of the flux at a point along the crystal, it should be a function of the distance from the cathode, the rate of acoustic gain and the magnitude of applied field. Using the attenuation constant  $\alpha$  derived by White (1962), which is given by:

$$\alpha = \frac{k^2}{4} \frac{\omega_m}{v_s} \frac{\delta}{\delta^2 + \frac{1}{4} \left[ \frac{\omega}{\omega_m} + \frac{\omega_m}{\omega} \right]^2} \quad (2.9)$$

where

$$\delta = \frac{1}{2} \frac{\omega_D}{\omega_m} \left[ \left( \frac{u}{u_s} - 1 \right) \right]$$

$$\omega_c = \frac{\sigma}{\epsilon}$$

$$\omega_m = (\omega_c \omega_D)^{1/2}$$

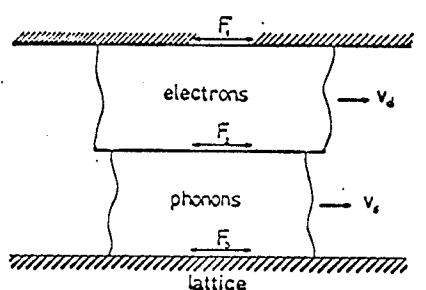


Fig. 1

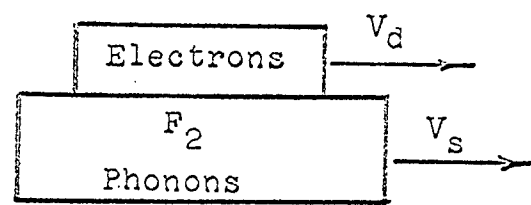


Fig. 3

### PHENOMENOLOGICAL MODEL OF ACOUSTOELECTRIC INTERACTION USED BY ROSE (1966)

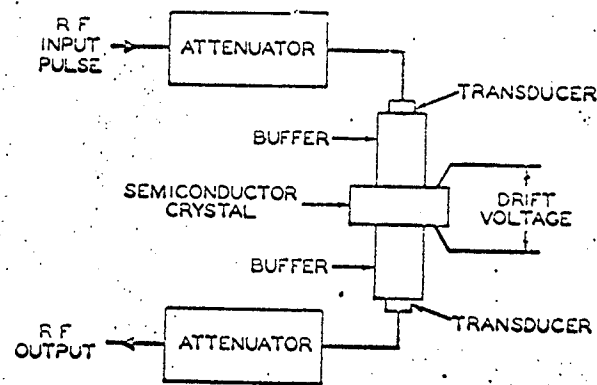


Fig. 2

### EXPERIMENTAL ARRANGEMENT USED BY

McFEE ET AL (1963)

$$\omega_D = \frac{V_S^2}{D}$$

$$D = \frac{kT\mu}{e}$$

2.10

$\epsilon$ , is the permittivity of the material; D, the diffusion constant; K, the Boltzmann constant; T, the absolute temperature. An implicit expression for the distance  $l_0$ , from the cathode to which electrons must travel under small signal gain conditions prior to the onset of acoustically induced negative differential conductivity, is given by Haydl (1967):

$$(2\alpha_m l_0)^{1/2} \exp(2\alpha_m l_0) = \left( \frac{8\pi^3 \epsilon kT}{\kappa^2 e^2 \alpha_l} \right) \exp(2\alpha_l l_0) \quad (2.11)$$

where  $\alpha_m$  is the rate of acoustic gain of the favoured band of random acoustic noise and  $\alpha_l$  is the corresponding lattice attenuation constant. The distribution of electric field as a function of distance,  $l$ , is shown in Fig. 4. It should be noted, however, that if the sample length is less than  $l_0$ , the domain formation will not occur.

What has been discussed so far applies only to small signal case. If an acoustic wave of large amplitude is present, all of the carriers are bunched in the troughs of the sound wave and are locked to the velocity of sound. The conditions given in Eqn. (2.10) cannot be satisfied. It is clear that once a significant number of carriers are locked in the potential well, the rate of doing work by the carriers on such a potential well is (Rose 1968):

$$\frac{dE}{dt} = ne(E - E_a) v_s \quad (2.12)$$

where  $E$  is the energy density of the sound wave and in which small signal approximation has not been used. The force  $neE$  tends to make the bunched carriers drift at the velocity of sound and the force  $ne(E - E_a)$  is transmitted by the carriers to the potential well when their velocity exceeds the velocity of sound. Space charge bunching in itself causes a further decrease in local resistivity and an increase in the local field external to the potential well. As a result, there is an increase in  $\frac{dE}{dt}$  resulting in further carrier bunching. A collective feedback process, terminated either by well collapse or by exhaustion of local carrier supply, is set in action.

Eqn. (2.11) is based on the assumption of a single coherent sound wave. In practice, however, a large number of frequencies exist, which form a noisy sound flux. In the case of sound waves with frequencies  $\omega_l$ , the electron density which is modulated by each wave can be expressed as:

$$n = n_0 + \sum_l n_l e^{j\omega_l t} + c_1 \quad (2.13)$$

and the corresponding drift velocity is:

$$v_d = v_0 + \sum_l v_l e^{j\omega_l t} + c_2 \quad (2.14)$$

and the current density is:

$$J = nev_d \quad (2.15)$$

where  $n_0$ ,  $n_l$  are the steady state component and varying

component of electron density, respectively;  $C_1$  and  $C_2$  are arbitrary constants. Substitution of Eqns (2.13) and (2.14) into Eqn. (2.15) gives:

$$\begin{aligned} J &= e n_0 v_0 + \left( e n_0 \sum_l v_l e^{j\omega_l t} + e v_0 \sum_l n_l e^{j\omega_l t} + \dots \right) \\ &\quad + \left( \sum_l e v_l n_l e^{j\omega_l t} \bar{e}^{j\omega_l t} \dots \right) + \left( \sum_{nm} e n_n v_m e^{j(\omega_n \pm \omega_m)t} \dots \right) \\ J &= J_0 + J(\omega_l) + J'(0) + J'(\omega_l) \end{aligned} \quad (2.16)$$

Prohofsky (1966) has shown that the piezoelectric non-linear interaction, represented by the third term in Eqn. (2.16) in the form of mixing currents at various frequencies, is quite strong in the usual crystals.

The approximate field-independent mean-life-time,  $t_m$ , of a potential domain (or well, as referred to in the previous discussion) should be expected to be equal to the sum of the mean incubation time,  $t_i$ ; the mean collapse time  $t_{co}$ ; and the mean-life-time in a saturated condition,  $t_{sc}$ .

$$t_m = t_i + t_{sc} + t_{co} \quad (2.17)$$

By analyzing Eqn. (2.17) two different non-linear effects due to electrons drifting through a homogeneous and infinite piezoelectric semiconductor become apparent. They are: (a) current saturation caused by the internal generation of acousto-electric current as a direct result of acoustic flux growth,

in this case  $t_i > t_{sc}$  and (b) negative differential conductivity caused by large carrier trapping in which  $t_i < t_{sc}$ .

#### 2.4 THE EFFECT OF TRAPS

Traps play a very important role in acoustoelectric current saturation in CdS. The condition for acoustoelectric current is:

$$E \mu_d = V_s \quad (2.18)$$

in which the mobility  $\mu_d$  can be interpreted as an effective drift mobility which is equal to  $f_0 \mu_H$ , where  $f_0$  is called the "trapping factor" taking into account the division of acoustically produced space charge between the conduction band and the bound states in the forbidden gap. Although the space charge bunching due to the presence of an acoustic wave can be neutralized by both bound and free charge, the resulting conductivity modulation which enables the d.c. field to feed energy into the sound wave (White 1962) can be effected only by free charge. Therefore, in the presence of traps, the applied field has to be increased to bring the free carrier concentration to equal that for the trap-free case, before the acoustoelectric effect can be observed.

In the presence of traps, the trap controlled drift mobility  $\mu_d$  and hall mobility  $\mu_H$  are related as:

$$\mu_d = \mu_H \frac{n}{n + n_t} \quad (2.19)$$

where  $n$ , is the density of free carriers and  $n_t$ , the density of trapped carriers. The acoustically produced space charge may be expected to divide in the same way between free and trapped states. Therefore:

$$\begin{aligned} f_0 &= \frac{N_d}{N_H} \\ &= \frac{1}{1 + \frac{n_t}{n}} \\ &= \frac{1}{1 + \tau_t/\tau_f} \end{aligned} \quad (2.20)$$

where  $\tau_f$  is the time during which the electron is free to move in the conduction band and  $\tau_t$  is the time the electron spends in a trap.

Assuming that there is a single trap level only as shown in Fig. 5, then  $f_0$  can be expressed as (Moore 1964):

$$f_0 = \left[ 1 + \left( \frac{N_t}{N_c} \right) e^{E_t/kT} \right]^{-1} \quad (2.21)$$

where  $N_t$  is the density of trapped carriers;  $N_c$ , the density of carriers in the conduction band; and  $E_t$ , the energy of the trapping level below the conduction band. The carrier velocity and current are given by:

$$V_s = N_d E_c = f_0 N_H E_c \quad (2.22)$$

and  $J = nev = neE\mu_H$

$$= \frac{neE N_d}{f_0} = (n+n_t) e E N_d \quad (2.23)$$

The saturation current is therefore:

$$J = J_{\text{sat}} = \frac{n e V_s}{f_0} = (n + n_t) e V_s \quad (2.24)$$

If the relaxation time  $\tau$  is assumed to be almost equal to  $\frac{1}{\omega}$  where  $\omega$  is the frequency of the sound wave (This means that the bound space charge produced by the acoustic wave equilibrates with the conduction band carriers in a time comparable to the period of the sound wave), there is a phase difference developed between the mobile and bound portions of the acoustically produced space charge and then  $f_0$  becomes a complex quantity  $f$ . Putting the total charge  $N$  as:

$$N = n + n_t \quad (2.25)$$

$f$  can be expressed as:

$$f = \frac{n}{n + n_t} = \frac{n}{N} \quad (2.26)$$

or

$$1-f = \frac{n_t}{N} \quad (2.27)$$

in which  $\frac{n}{\tau_f}$  = the charge set free per second.

$\frac{n_t}{\tau_t}$  = the charge trapped per second

$\frac{n}{\tau_f} - \frac{n_t}{\tau_t}$  = rate of change of trapped charge

$$= \frac{dn_t}{dt} \quad (2.28)$$

Assuming that the total charge varies sinusoidally

$$N = N_0 e^{j\omega t} \quad (2.29)$$

then from Eqn. (2.28)  $f$  can be written in the form:

$$f = \frac{T_f (1 + j\omega T_f)}{T_f + T_t + j\omega T_t T_f} \quad (2.30)$$

Setting

$$\tau = \frac{T_t T_f}{T_f + T_t}$$

Eqn. (2.30) becomes:

$$f = \frac{f_0 + j\omega\tau}{1 + j\omega\tau} \quad (2.31)$$

or

$$f = \frac{bf_0}{1 - ia}$$

where

$$a = \frac{(1 - f_0)\omega\tau}{f_0 + \omega^2\tau^2}$$

and

$$b = \frac{f_0^2 + \omega^2\tau^2}{f_0(f_0 + \omega^2\tau^2)}$$

By neglecting carrier diffusion due to space charge bunching, the current density in a piezoelectrical semiconductor can be expressed as:

$$J = q\mu_d [n(x) + f n_s(x)] \cdot [E_0(x) + E_1(x)] \quad (2.32)$$

where  $E_1$  is the alternating component of the electric field;  $E_0$ , the steady state component of the electric field; and  $n_s$ , the density of carriers in the space charge. The steady state component in Eqn. (2.32) is given by:

$$J_{d.c.} = q\mu_d n(x) E(x) + qN_d \cdot \frac{1}{2} \operatorname{Re}(f n_s E_1^*) \quad (2.33)$$

the second term is the acoustoelectric current,

$$J_a = qN_d \cdot \frac{1}{2} \operatorname{Re}(f n_s E_1^*) \quad (2.34)$$

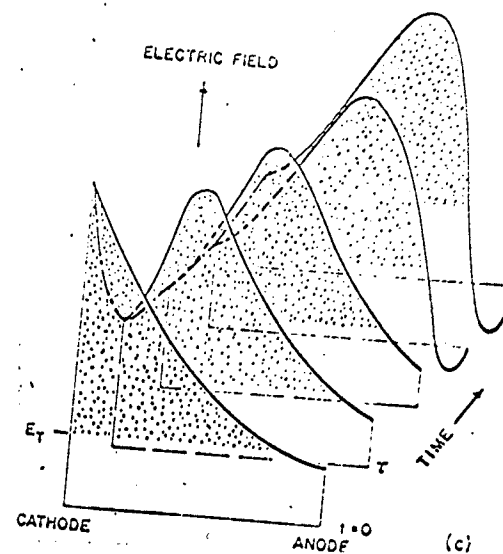


Fig. 4. THE DISTRIBUTION OF ELECTRIC FIELD AS A FUNCTION OF DISTANCE (HAYDL, 1967).

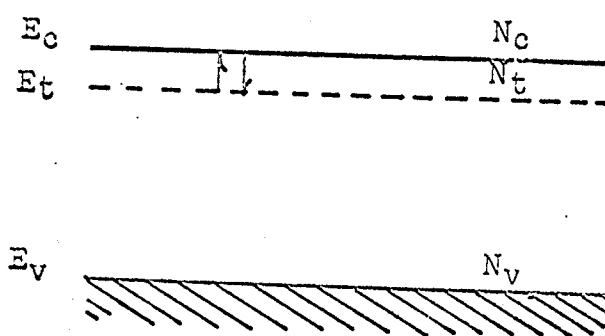


Fig. 5 ENERGY LEVEL DIAGRAM WITH A SINGLE TRAP LEVEL

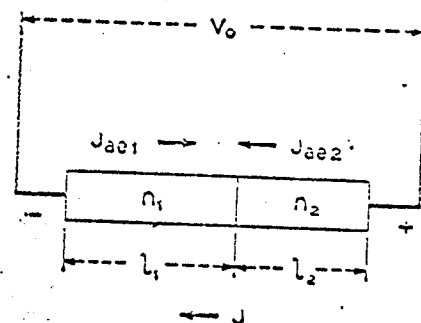


Fig. 6. MODEL OF AN INHOMOGENEOUS SAMPLE

Since  $f$  is a complex quantity, it can be expressed as:

$$f = f_R - j f_I \quad (2.35)$$

Thus Eqn. (2.34) becomes:

$$\begin{aligned} J_a &= q\mu_d \cdot \frac{1}{2} \operatorname{Re} [f_R \cdot n_s E_i^* - j f_I n_s E_i^*] \\ &= \frac{1}{2} q\mu_d f_R \cdot \operatorname{Re}(n_s E_i^*) - \frac{1}{2} q\mu_d f_I \operatorname{Im}(n_s E_i^*) \end{aligned} \quad (2.36)$$

At the threshold field for saturation, the first term on the right-hand side of Eqn. (2.36) can be expressed as:

$$\begin{aligned} \frac{1}{2} q\mu_d \cdot f_R \cdot \operatorname{Re}(n_s E_i^*) &= \frac{1}{2} q\mu_d f_R \cdot \operatorname{Re}\left(-\frac{J_1 E_i^*}{q v_s}\right) \\ &= -f_R \left(\frac{\mu_d}{v_s}\right) \cdot \frac{1}{2} \operatorname{Re}(J_1 E_i^*) \end{aligned} \quad (2.37)$$

since  $J_1 = -q v_s n_s$ . Under this condition, the power absorbed or delivered by the carriers is equal to the rate at which acoustic energy decreases (or increases). Therefore,

$$\frac{1}{2} \operatorname{Re}(J_1 E_i^*) = 2\alpha \phi = \frac{dU}{dt} \quad (2.38)$$

where  $U$  is the acoustic energy density, and  $\phi$ , the acoustic flux. Introducing these in Eqn. (2.34)  $J_a$  is given by:

$$J_a = -f_R \left(\frac{\mu_d}{v_s}\right) \cdot 2\alpha \cdot \phi - \frac{1}{2} q\mu_d f_I \operatorname{Im}(n_s E_i^*) \quad (2.39)$$

From Eqn. (2.31)  $f_R$  and  $f_I$  can be expressed as:

$$\begin{aligned} f_R &= b f_0 / (1 + a^2) \\ f_I &= -a b f_0 / (1 + a^2) \end{aligned} \quad (2.40)$$

Of course, if  $f$  is a real quantity, Eqn. (2.39) becomes:

$$J_a = -f_R \left( \frac{N_d}{V_s} \right) (2\alpha) \cdot \phi \quad (2.41)$$

This equation is known as Weinreich's relation (McFee, 1966).

Substituting the results for  $n_s$  and  $E_1$  in Eqn (2.41) (McFee, 1966), we get

$$J_a = -N_d \frac{\omega_c e^2}{V_s \epsilon} \times S_1^2 \left\{ \frac{bf_0 \gamma'}{\left[ \gamma' - \alpha \left( \frac{\omega_c}{\omega} \right)^2 + \left( \frac{\omega_c}{\omega} \right) + \left( \frac{\omega}{\omega_D} \right) + \alpha \right]} \right\} \quad (2.42)$$

Where  $\gamma' = 1 + (bf_0 N_d E_{dc}/V_s)$ ,  $S_1$  is a constant.

The attenuation constant  $\alpha$  in the presence of trapping becomes

$$\alpha = \frac{\omega_c}{V_s} \frac{e^2}{2c\epsilon} \left[ \frac{\gamma' + \alpha \left[ (\omega/\omega_D) + \alpha \right]}{\left[ \gamma' - \alpha \left( \omega_c/\omega \right) \right]^2 + \left[ \left( \frac{\omega_c}{\omega} \right) + \left( \frac{\omega}{\omega_D} \right) + \alpha \right]^2} \right] \quad (2.43)$$

This can compare with Eqn. (2.9) for the trap-free case.

## 2.5 THE EFFECT OF NON-HOMOGENEITY

All samples prepared for the study of acousto-electric interactions are, to a certain extent, non-homogeneous. However, in here we discuss two possible cases as follows:

### (A) HOMOGENEOUS SAMPLES:

The attenuation constant  $\alpha$  of an acoustic wave in a piezoelectric material can also be written as (White 1962, see also Eqn. 2.18)

$$\alpha \frac{V_s}{\omega} = \frac{k^2}{2} \frac{\omega_c / \gamma \omega}{1 + \frac{\omega_c^2}{\gamma^2 \omega^2} \left( 1 + \frac{\omega^2}{\omega_c \omega_D} \right)} \quad (2.44)$$

The maximum gain occurs when

$$-\gamma = \frac{\omega_c}{\omega} + \frac{\omega}{\omega_D} = \frac{\omega_c}{\omega} \left[ 1 + \frac{\omega^2}{\omega_c \omega_D} \right] \quad (2.45)$$

$$\omega = \omega_m = (\omega_c \omega_D)^{1/2}$$

$$\begin{aligned} -\gamma &= \frac{2\omega_c}{(\omega_c \omega_D)^{1/2}} \\ &= 2 \left( \frac{\omega_c}{\omega_D} \right)^{1/2} \end{aligned} \quad (2.46)$$

Substituting Eqn. (2.45) in Eqn. (2.44) we get

$$\alpha_m \frac{V_s}{\omega} = \frac{k^2}{2} \frac{\omega_c / \gamma \omega}{1 + \frac{\omega_c}{\gamma \omega}} = \frac{k^2}{2} \frac{1}{\frac{\gamma \omega}{\omega_c} + 1} \quad (2.47)$$

Where  $\alpha_m$  is the value of  $\alpha$  for maximum gain condition

substituting Eqn. (2.46) into the above Eqn. gives

$$\alpha_m \frac{V_s}{\omega} = \frac{k^2}{2} \frac{1}{2 \left( \frac{\omega_c}{\omega_D} \right)^{1/2} \frac{(\omega_c \omega_D)^{1/2}}{\omega_c}} = \frac{k^2}{4}$$

or

$$\begin{aligned} \alpha_m &= \frac{k^2}{4} \frac{\omega}{V_s} = \frac{k^2}{4} \frac{(\omega_c \omega_D)^{1/2}}{V_s} = \frac{e^2}{4C\epsilon} \frac{V_s^2 \sigma}{D^{1/2} \epsilon V_s} \\ &= \frac{e^2}{4C\epsilon^2} \frac{\sigma e^{1/2}}{(\mu k T)^{1/2}} \frac{1}{V_s} \propto \frac{\sigma}{\mu^{1/2}} \end{aligned} \quad (2.48)$$

Therefore  $\alpha_{max}$  is directly proportional to  $\frac{\sigma}{\mu^{1/2}}$ . This implies that if the conductivity is low, it will take a longer time (i.e.  $t_i > t_{sc}$ ) for domain to build up and a convective bunching may not take place, thus hindering the occurrence of acoustoelectric instability. On the other hand, if the conductivity is high, there may be oscillation in the crystal.

(B) NON-HOMOGENEOUS SAMPLES:

Suppose that a sample of low gain is composed of two homogeneous portions 1 and 2 to form an inhomogeneous sample Fig.6; the carrier concentration in portion 1 being greater than that in portion 2. When a voltage  $V$  is applied to such a sample, the field in portion 1 will exceed that in portion 2. At a critical field when there is an acoustic gain in portion 1 and an acoustic attenuation in portion 2, there will be a growth of acoustic waves in the high field region and an electronic damping of acoustic waves in the low field region. Thus, in portion 1, the acoustoelectric field is opposite to the drift current and in portion 2, it is in the direction of the drift current. By assuming that all the acoustic energy build-up in portion 1 is taken away by the electronic system in portion 2, the current through the sample can be written as:

$$J = n_1 q \mu_d E_1(x) - J_{a1} \quad (2.49)$$

$$J = n_2 q \mu_d E_2(x) - J_{a2} \quad (2.50)$$

Where  $J_{a1}$  is the acoustoelectric current in portion 1 and  $J_{a2}$  is the acoustoelectric current in portion 2,  $n_1$  and  $n_2$  are the densities of carriers in portion 1 and portion 2, respectively. From Weinreich's relation (Eqn. 2.41)

$$J_a = -f_R \left( \frac{\mu_d}{V_s} \right) \cdot 2\alpha \cdot \phi = -f_R \left( \frac{\mu_d}{V_s} \right) \frac{dV}{dt} \quad (2.51)$$

By substituting Eqn. (2.51) into Eqns. (2.49) and (2.50) and integrating over each part of the sample, we obtain

$$J_{l_1} = -n_1 q_1 \mu_d E_1 l_1 - f_R \left( \frac{\mu_d}{V_s} \right) \int_0^{l_1} \frac{dV}{dt} dl \\ = -\sigma_1 V_1 - f_R \left( \frac{\mu_d}{V_s} \right) \frac{d\phi_1}{dt} \quad (2.52)$$

and

$$J_{l_2} = -\sigma_2 V_2 - f_R \left( \frac{\mu_d}{V_s} \right) \left[ - \int_{l_1}^{l_1 + l_2} \frac{dV}{dt} dl \right] \\ = -\sigma_2 V_2 + f_R \left( \frac{\mu_d}{V_s} \right) \frac{d\phi_1}{dt} \quad (2.53)$$

where  $l_1$  and  $l_2$  are the lengths of portion 1 and portion 2, respectively. Thus the applied voltage  $V_o$  is

$$V_o = V_1 + V_2 = \frac{f_R \mu_d}{V_s} \left( \frac{1}{\sigma_1} - \frac{1}{\sigma_2} \right) - J \left( \frac{l_1}{\sigma_1} + \frac{l_2}{\sigma_2} \right) \quad (2.54)$$

and the total current is

$$I = AJ = -\frac{V_o}{R_1 + R_2} + \frac{\mu_d / V_s \left( \frac{1}{\sigma_1} - \frac{1}{\sigma_2} \right) \left( \frac{d\phi_1}{dt} \right)}{R_1 + R_2} \quad (2.55)$$

where  $A$  is the area of the electrode since  $\sigma_1 < \sigma_2$ ,

Thus when  $\frac{d\phi_1}{dt} > 0$  i.e. there is a growth flux,  $|I|$  will be reduced below its ohmic value and acoustoelectric saturation will result. The inhomogeneity in the sample helps the growth of the acoustoelectric effect.

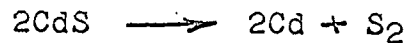
## CHAPTER 3

FABRICATION OF CdS FILMS AND  
EXPERIMENTAL TECHNIQUES

There are at least four very important factors for which care must be taken in the deposition of thin films:

- (1) Residual gas pressure.
- (2) Substrate temperature.
- (3) Evaporation rate.
- (4) Cleanliness of the substrate and the purity of the material.

In the present investigation, the residual gas pressure at the time of evaporation was maintained between  $4 \times 10^{-6}$  -  $10^{-5}$  Torr., with the substrate temperature of  $200^{\circ}\text{C} \pm 3^{\circ}\text{C}$ . It was found that CdS dissociated into its constituent elements at its evaporation temperature



If CdS film is fabricated by evaporation in vacuum in an ideal system in which there is a finite distance between the source and the substrate, a film would contain not just CdS, but also Cd and S. To minimize the content of Cd and S, the evaporation rate is a very important factor which depends upon the source temperature, the residual gas pressure and the type

of source. A slower evaporation rate or lower source temperature would reduce the possibility of dissociation of CdS, so that the source temperature used was 500°C (The temperature for dissociation of CdS at a pressure of  $10^{-6}$  torr is 750°C (Deklerk and Kelly 1965) . The films so produced were then heat-treated to minimize any non-homogenities in it.

The reaction of CdS with other active elements present in the system during evaporation was avoided by cleaning the system properly and flushing it with Argon gas before pumping the system. The substrate holder, the cylinder through which the CdS vapour passed through before depositing on the substrate and the source material were degassed for 20 minutes at about 300°C under vacuum. A residual gas pressure of  $4 \times 10^{-6}$  torr was then maintained before evaporation of CdS.

The substrates were cleaned using the following procedure:

- (1) Cleaning in concentrated HCl for 5 min.
- (2) Ultrasonic cleaning in Alconox for 3 min.
- (3) Washing with hot chromic acid.

The substrate was rinsed with deionized water between each stage. The clean substrates were stored in an isopropyl alcohol vapour bath.

### 3.1 FABRICATION TECHNIQUE

The substrates were baked at 300°C for at least one hour in vacuum before deposition and then cleaned by ion

bombardment for 10 minutes. A baffled source was used for evaporation in order to avoid any foreign particles to be thermally ejected to reach the substrate. Deposition was carried on for 45 minutes on sapphire substrates which were kept at a temperature of  $200^{\circ}\text{C} \pm 3^{\circ}\text{C}$ . A continuous evaporation for 45 minutes yielded a film of thickness of 1 micron. When the system cooled down to  $30^{\circ}\text{C}$ , it was exposed to atmosphere. The evenly deposited films were taken out and stored in a dessicator for heat-treatment.

The films deposited by the above technique showed low mobility ( $1-30 \text{ cm}^2/\text{v sec.}$ ) as compared to  $200-250 \text{ cm}^2/\text{v sec}$  in bulk crystals and low photoconductivity (i.e. low photocurrent to dark current ratio). In order to compensate for the stoichiometricity and to recrystallize the structure, The films were heat-treated using the method of Böer et. al. (1965) at  $620^{\circ}\text{C}$  in the presence of CdS powder, Cu, HCl vapour and  $\text{O}_2$ , each of which having a major role to play in improving the mobility and photoelectric properties of the film.

### 3.2 POST-EVAPORATION HEAT-TREATMENT OF Cds FILMS

Various methods (Berger, 1961 and Dresner, 1963 etc.) have been used to improve and to control the properties of evaporated CdS films. For obtaining c-axis oriented films of high mobility, the films have been doped with a range of dopants. Some experimenters (DeKlerk 1965, Foster 1966, etc.) have tried to add a desired amount of dopant to the CdS powder used for evaporation or to coat the deposited films with a dopant film

(such as In on CdS) and then to allow sufficient time for the dopant to diffuse into the CdS film. But none of these methods have been adequately standardized and then remain as an art with the experimenters.

Gilles and Van Cakenberghe (1963) used Ag and Cu as dopants and found that the presence of oxygen in the firing environment increased the crystallization rate and size of the crystalline portions 3 to 4 times. Dresner and Shallcross (1963) treated the films with Cu, Ag, In and Ga, and confirmed that the presence of oxygen accelerated the crystallization. In an attempt to remove the sulphur vacancies, they annealed the films in sulphur vapour with a fair amount of success.

Some post-evaporation heat-treatments seem to contribute significantly to crystalline growth and reducing the lattice strains. Berger et.al. (1963) have reported that heat-treatments in vacuum or in different gas atmospheres as Argon, Nitrogen and Oxygen resulted in crystalline growth.

### 3.2.1 METHOD OF HEAT-TREATMENT

Bohr's method for post-evaporation heat-treatment was found to be the most promising one for the facilities available in our laboratory. This method was designed to:

- (1) reduce the native astoichiometricity in the film.
- (2) compensate for the sulphur vacancies with Cu and Cl.
- (3) increase the rate of recrystallization in the presence of oxygen.

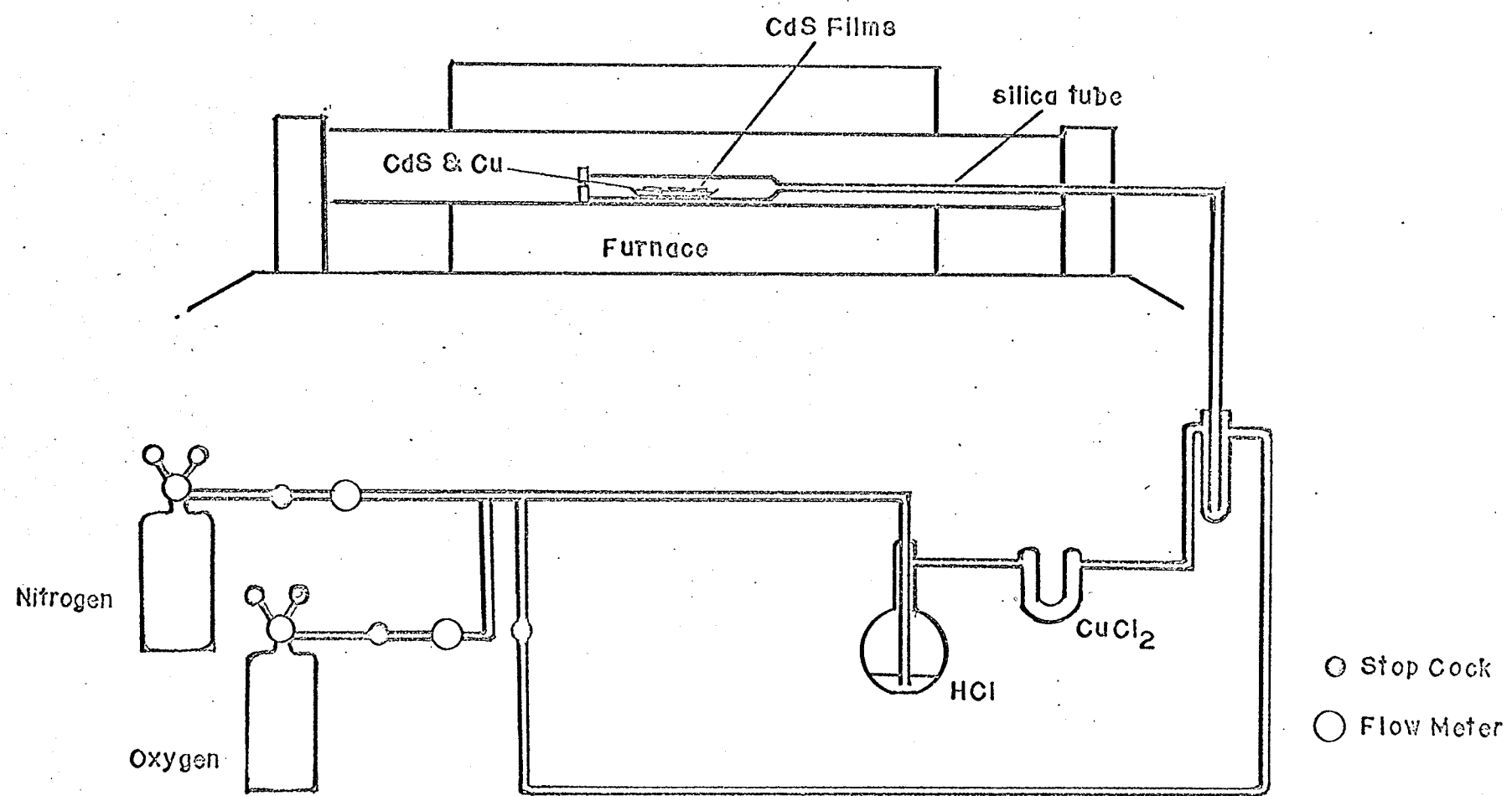


Fig. 7 HEAT TREATMENT OF CdS FILMS

33

(4) release the lattice strains by thermal annealing.

The set-up used for heat-treatment is shown in Fig.7. 15 grams of CdS powder mixed with 2.0 grams of copper powder (99.999% pure) were kept in a quartz boat and 3 films of CdS deposited on sapphire substrate were placed one next to the other along its length. All the glass tubings used in the set-up were thoroughly cleaned with chromic acid and acetone before heat-treatment. The furnace temperature was maintained at  $630^{\circ}\pm 10^{\circ}\text{C}$  which was constantly checked using a Cromel Alumel thermocouple. The boat was placed in the middle of the quartz tube. After closing the end of the tube with a ceramic cork, it was placed in the furnace and immediately connected to the nitrogen supply. A flow rate of about 3600 c.c./min. was maintained for about 10 minutes when the HCl and oxygen supplies for  $250 \pm 50$  c.c./min. and 10 c.c./min. respectively were connected. The heat-treatment was carried out for about 40 minutes. Then the oxygen and HCl supplies were turned off and the quartz tube was allowed to cool down to  $150^{\circ}\text{C}$  under a nitrogen atmosphere. Further cooling to room temperature was done outside the furnace in nitrogen atmosphere. The heat-treated films were inspected, and those with signs of peeling off, and discolouration were discarded. Good samples were stored in a chamber under a vacuum of  $10^{-3}$  torr. The thickness of the film used for the present investigation was found to be 1.2 micron. The thickness was estimated by weighing the substrate with a micro-balance before and after the deposition of CdS and by measuring

the area of the deposit. The thickness of the film was then confirmed using an interferometer. To use this method, a layer of a metal (such as silver) was deposited on one of the four sides of the film so as to form a step with the substrate Fig. 9. The interferometer measures the height of this step which is equal to the thickness of the film. These two methods give closely agreeable results on film thickness measurement.

### 3.2.1 EFFECTS OF HEAT-TREATMENT

The heat-treatment increased the size of the crystallites and the photo-conductivity of the films. The c-axis of the film is perpendicular to the substrate whose c-axis is also perpendicular to its surface. Published literature on the structure and orientation of CdS films reveals that the films are polycrystalline, predominantly hexagonal in phase and are c-axis oriented. The post-evaporation heat-treatments show tilts of up to  $25^\circ$  in the c-axis of the crystallites (Foster, 1966) which is thought to be their minimum energy configuration. Since the post-evaporation heat-treatment increases the mobility of carriers considerably, the tilt in the c-axis does not affect the acoustoelectric interactions in the film very much. X-ray diffraction studies show that the crystallites are oriented in one direction Fig. 8. Since the films may contain a considerable amount of cubic phase which cannot be detected by x-ray or electron diffraction techniques, therefore it is difficult to define the orientation of films.

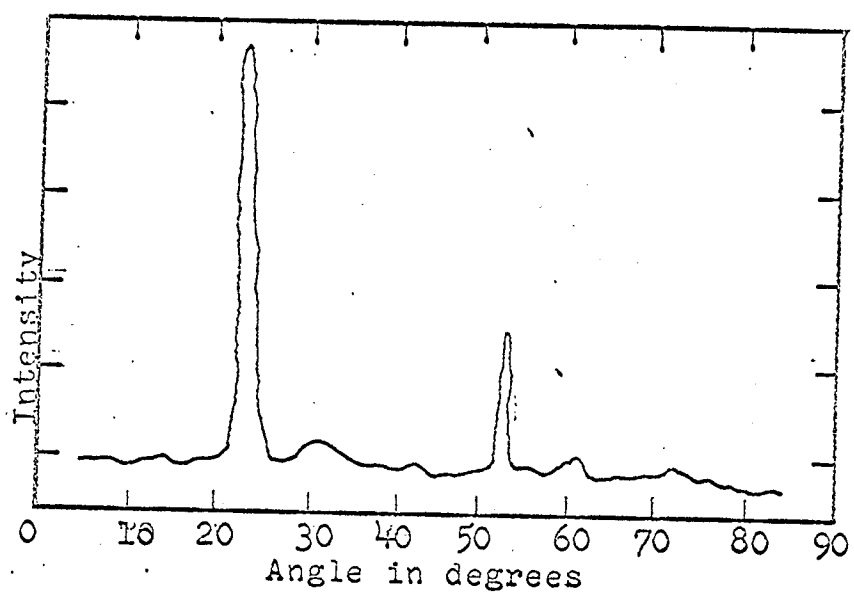


Fig. 8: X-RAY DIFFRACTION PATTERN

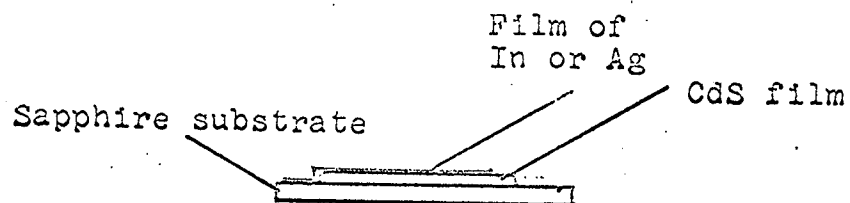


Fig. 9: SAMPLE FOR THICKNESS MEASUREMENT

It can be concluded that the heat-treatment does anneal out certain structural defects which get stabilized in the film due to the rapid diffusion of impurities incorporated during firing. A considerable number of astiochiometries can be expected in the neighbourhood of these structural defects. The thermodynamically unstabilized film can be viewed upon as a complex mesh structure of resistors and junctions that can short circuit, open circuit or forbid conduction in certain directions of the film, which may give rise to a low carrier mobility. Heat-treatments loosen (anneal out) these structural disorders (Thermodynamic stabilization).

### 3.2.2 OHMIC CONTACTS

The successfully heat-treated films were mounted in the sample holder. High purity Indium metal was then deposited on the film at a temperature of  $100^{\circ}\text{C}$  in a nitrogen atmosphere at a pressure of  $4 \times 10^{-6}$  torr. 90% of the contacts made this way were found to be ohmic. However, post-evaporation heat-treatment in air at  $70^{\circ}\text{C}$  for 10 minutes improved further the ohmic behaviour, and sometimes could make the other 10% which are not quite ohmic before, ohmic.

## CHAPTER 4

## EXPERIMENTAL RESULTS AND DISCUSSION

## 4.1

The unavoidable level of native and foreign defects play a dominant role in the conduction process in a CdS film at high fields. The high resistivity CdS acts as a dielectric between two neighbouring impurities and the electrons travel from one impurity site to the other causing a breakdown which shows up in the form of scratches on the film at high fields Fig.10. As a precaution against surface breakdown, the width of the film was reduced to 2mm. The breakdown was attributed to the surface impurities and occurred in many of the good heat-treated films. After reducing the width and shining light of high intensity on the film, the breakdown voltage increased considerably.

The sample was mounted in a holder specially designed for low temperature experiments, as shown in Fig.12. The sample was partially shaded by a 50% transmission Kodak wratten filter to make the carrier concentration non-uniformly distributed (or non-uniformly resistive). To avoid heating the sample, rectangular pulses of  $50\text{ }\mu\text{Sec}$ .duration (The design of the pulse generator is given in Appendix) were used to measure the V-I characteristics. The circuit used is shown in Fig. 11. Under very strong illumination, the photocurrent is about three orders of magnitude higher than the dark current as shown in Fig. 18.

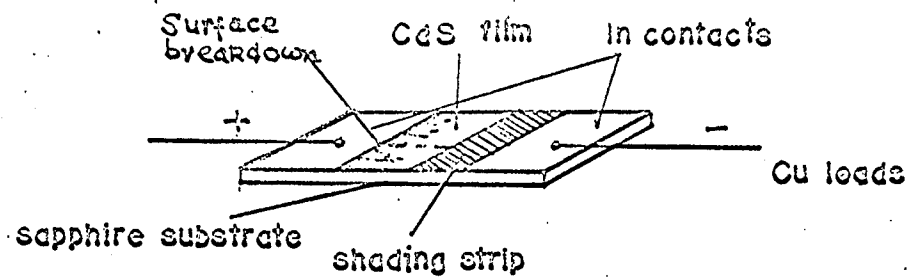


Fig. 10 SAMPLE GEOMETRY (Size 0.8×0.65 cm)  
AND SURFACE BREAKDOWN

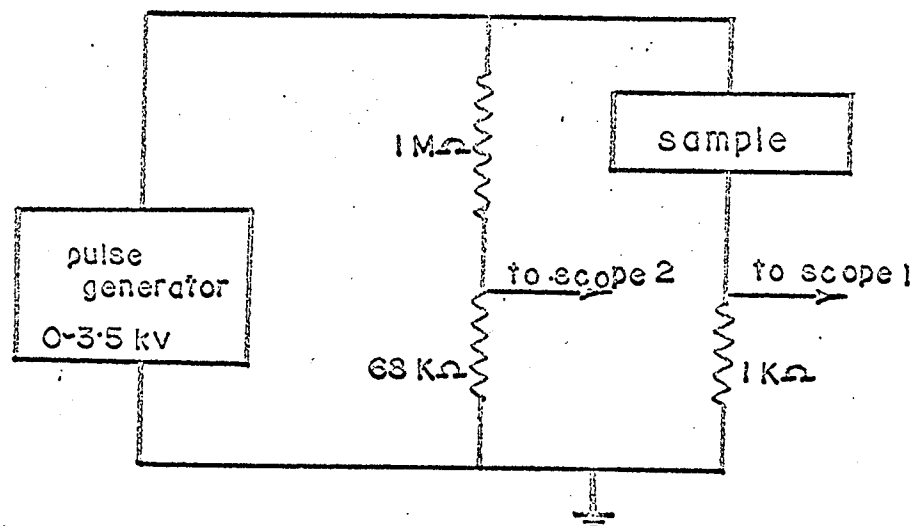


Fig. 11 CIRCUIT DIAGRAM

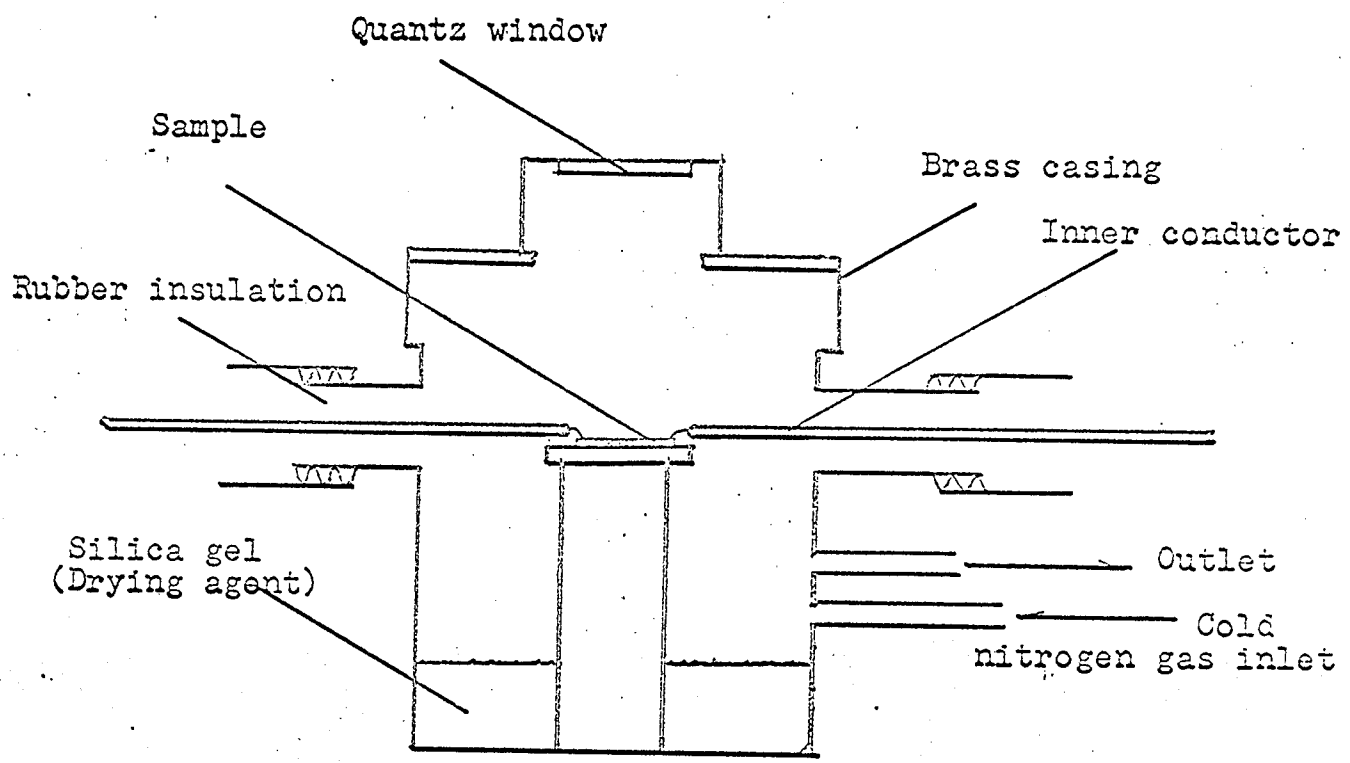
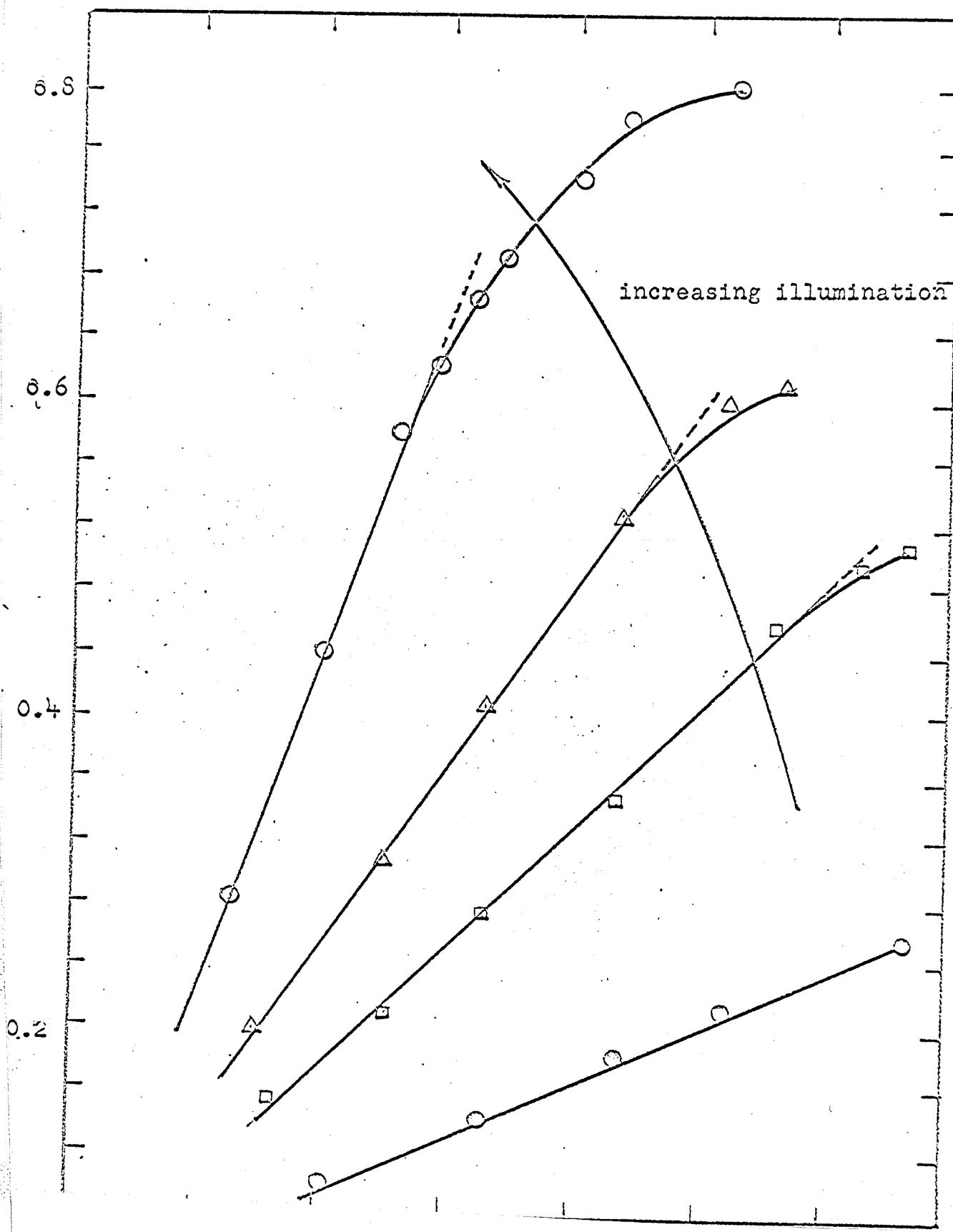


Fig.12.SAMPLE HOLDER



In one good sample the current saturation occurs at a field of about 5.0 kV/cm. The saturation current increases with increasing illumination, but the threshold field for current saturation decreases with increasing illumination as shown in Fig. 13.

In order to study the effect of gamma-ray radiation on the acoustoelectric current saturation in CdS films, a sample was irradiated with gamma-rays for 10 min. and its V-I characteristics were measured. The above procedure was repeated till there was no current saturation observed. Increasing the voltage to make sure that there was no saturation at higher fields caused surface breakdown. Fig. 17 shows a plot of photocurrent at five radiation doses. It could be seen that:

- (i) The photocurrent decreases with increasing the time for which the sample was irradiated with gamma-rays.
- (ii) The threshold field for current saturation increases with increasing the time of irradiation.

The irradiator used for the above study was a Cobalt 60 irradiator with a dose rate of  $1.6 \times 10^6$  rads/hr. measured with ferrous sulphate on May 6<sup>th</sup> 1966. The dose rate at the time of the experiment was 0.9028 rads/hr. (calculated by using the table provided with the above equipment). The radiation dose for each 't' min. would then be equal to  $0.9028 \times 10^6 \frac{xt}{60}$ .

#### 4.2 DISCUSSION

Current saturation and oscillation in bulk piezoelectric semiconductors have been discussed at length by many investigators. However, little has been reported on the same phenomenon in films.

Fig. 14 shows that the photocurrent decreases with increasing temperature. On the assumption that the carrier concentration remains constant, the carrier mobility can be calculated using the method suggested by Hamaguchi et.al. (1964).

$$\mu_d E_{th} = v_s \quad (4.1)$$

where  $E_{th}$  is the threshold field for current saturation and  $v_s$  is the velocity of sound ( $4.4 \times 10^5$  cm/sec.). Knowing the threshold field for current saturation at  $300^\circ K$  and  $153^\circ K$  and assuming that the velocity of sound does not change with temperatures,\* the carrier mobilities were calculated to be  $80 \text{ cm}^2/\text{v-sec}$  at  $300^\circ K$  and  $100 \text{ cm}^2/\text{v-sec}$  at  $153^\circ K$ . The low mobility in films explains why the threshold field for the onset of current saturation in films is much higher than that in crystals.

The photocurrent beyond the onset point still increases very slowly with increase of applied field; but when the field is further increased, there is another onset point at which the current suddenly changes very abruptly as shown

\* A general simple formula for the velocity of sound in a material with modulus of elasticity  $E_m$  and density  $\rho$  is given by;

$$v_s = \sqrt{\frac{E_m}{\rho}}$$

Since the ratio  $\frac{E_m}{\rho}$  does not change very much with change in temperatures the above assumption is fairly accurate.

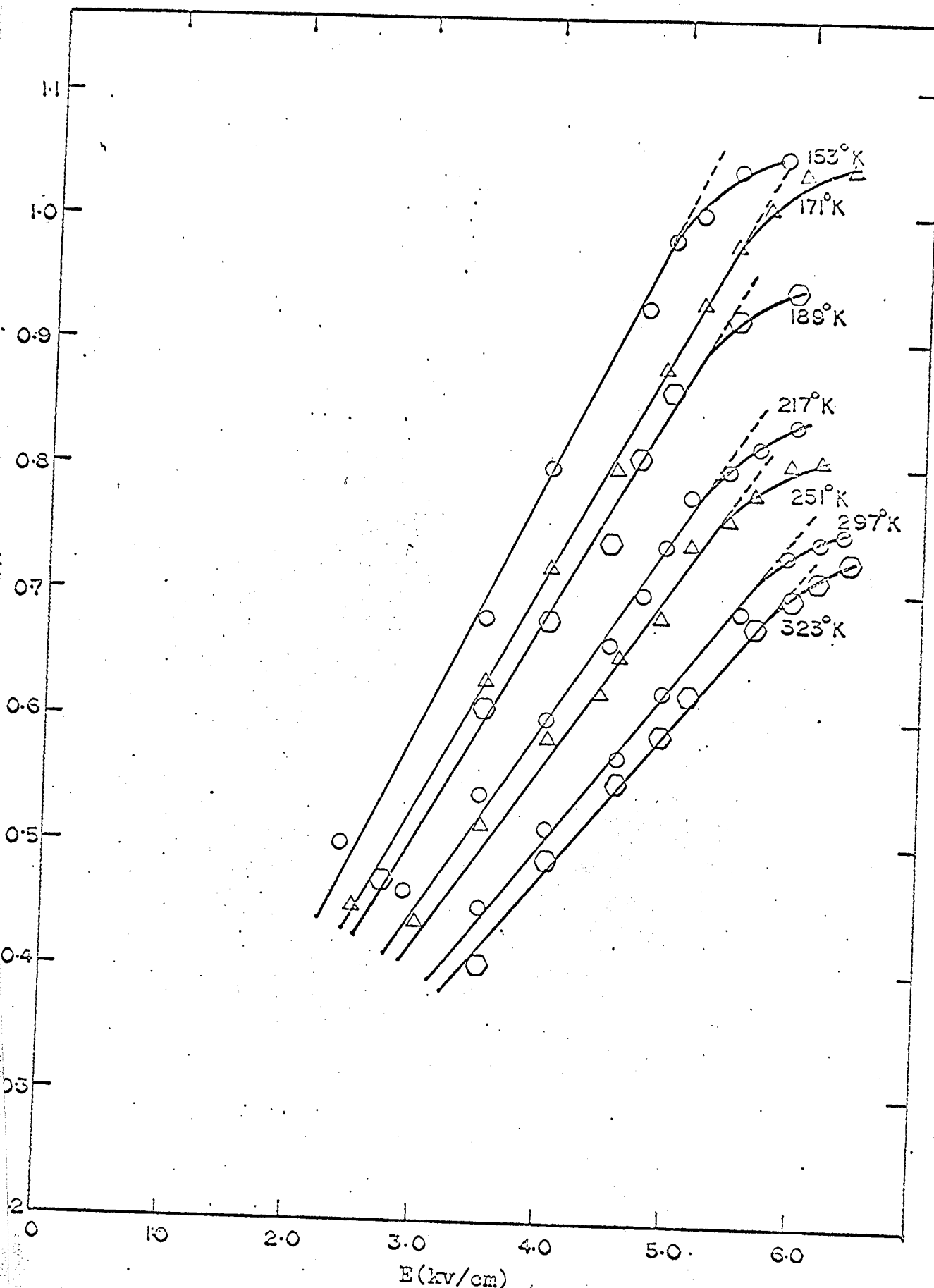


Fig. 14 PHOTOCURRENT AS A FUNCTION OF ELECTRIC FIELD AT VARIOUS TEMPERATURES

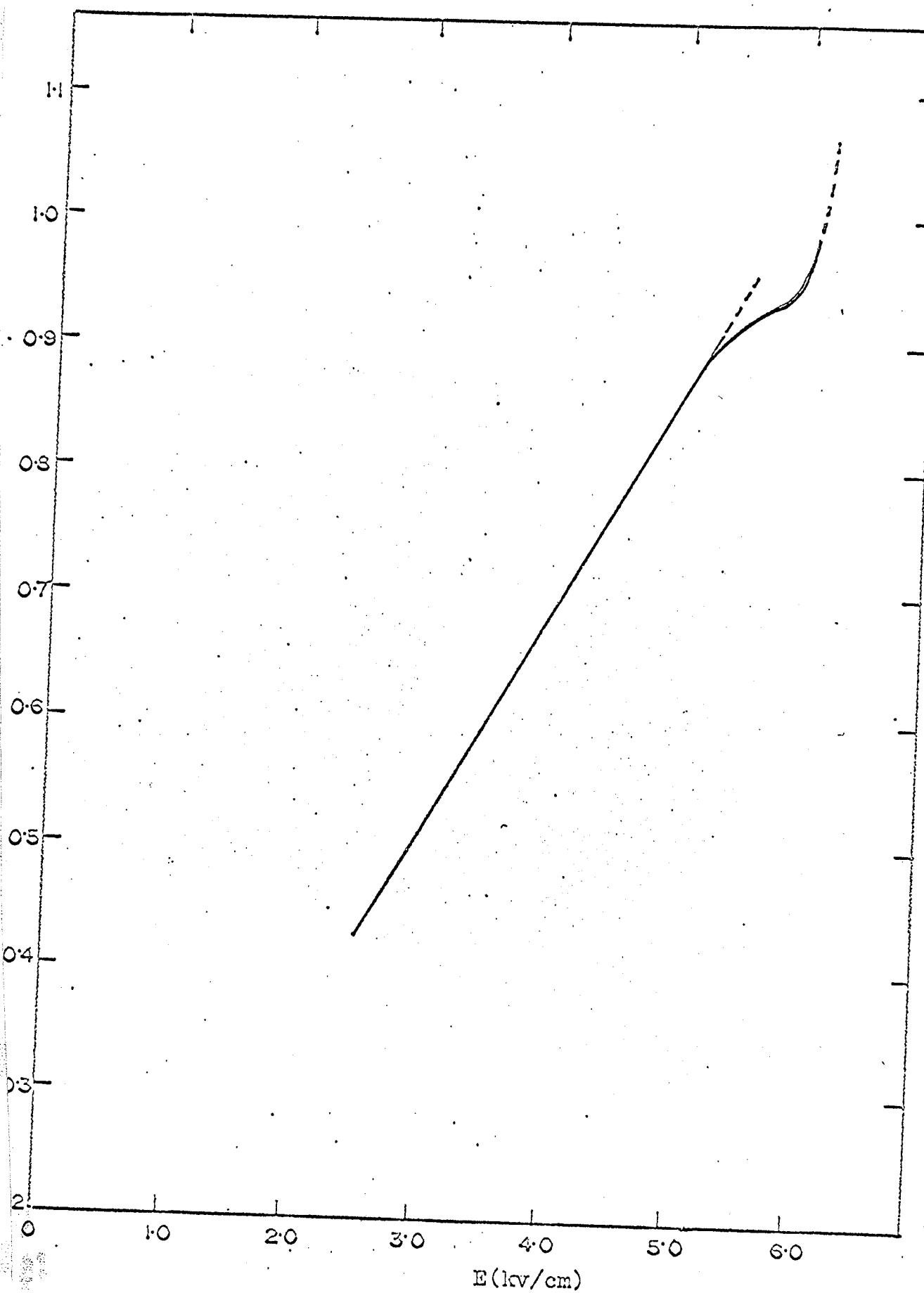


Fig.15 THE VARIATION OF PHOTOCURRENT WITH FIELD AT  $189^{\circ}\text{K}$  FOR FIELDS LARGER THAN THE THRESHOLD FOR SATURATION

in Fig. 15. This may indicate that the field corresponding to the second onset point approaches the breakdown strength of the film.

There are two possible mechanisms which may give rise to current saturation in CdS films, and they are: (a) field enhanced trapping, and (b) acoustic wave interaction with free carriers. These two mechanisms have been distinguished in the light of the experimental facts as follows:

(i) The saturation photocurrent decay time was measured to be of the order of  $2-3\mu\text{sec}$ . The decay time of the pulse applied to the sample is of the order of  $2\mu\text{sec}$  and the decay time of the current pulse observed below the threshold is of the order of  $2\mu\text{sec}$ . Above the threshold for current saturation there was no significant change in the decay time of the current pulse. This invalidates mechanism (a) since the carrier de-trapping time would be of the order of  $0.5\text{ msec}$  (Mason 1968, Moore 1964).

(ii) For mechanism (a) the higher the applied field, the more would be the carriers trapped; and this trapping process would be enhanced at low temperatures, and then the photocurrent would be expected to decrease with decreasing temperature. But this contradicts the results given in Fig. 14.

(iii) The threshold field for the onset of photocurrent saturation increases linearly with increasing temperatures as shown in Fig. 16, indicating that the carrier drift velocity is larger than the velocity of acoustic surface waves, the latter is, in fact, the required condition for

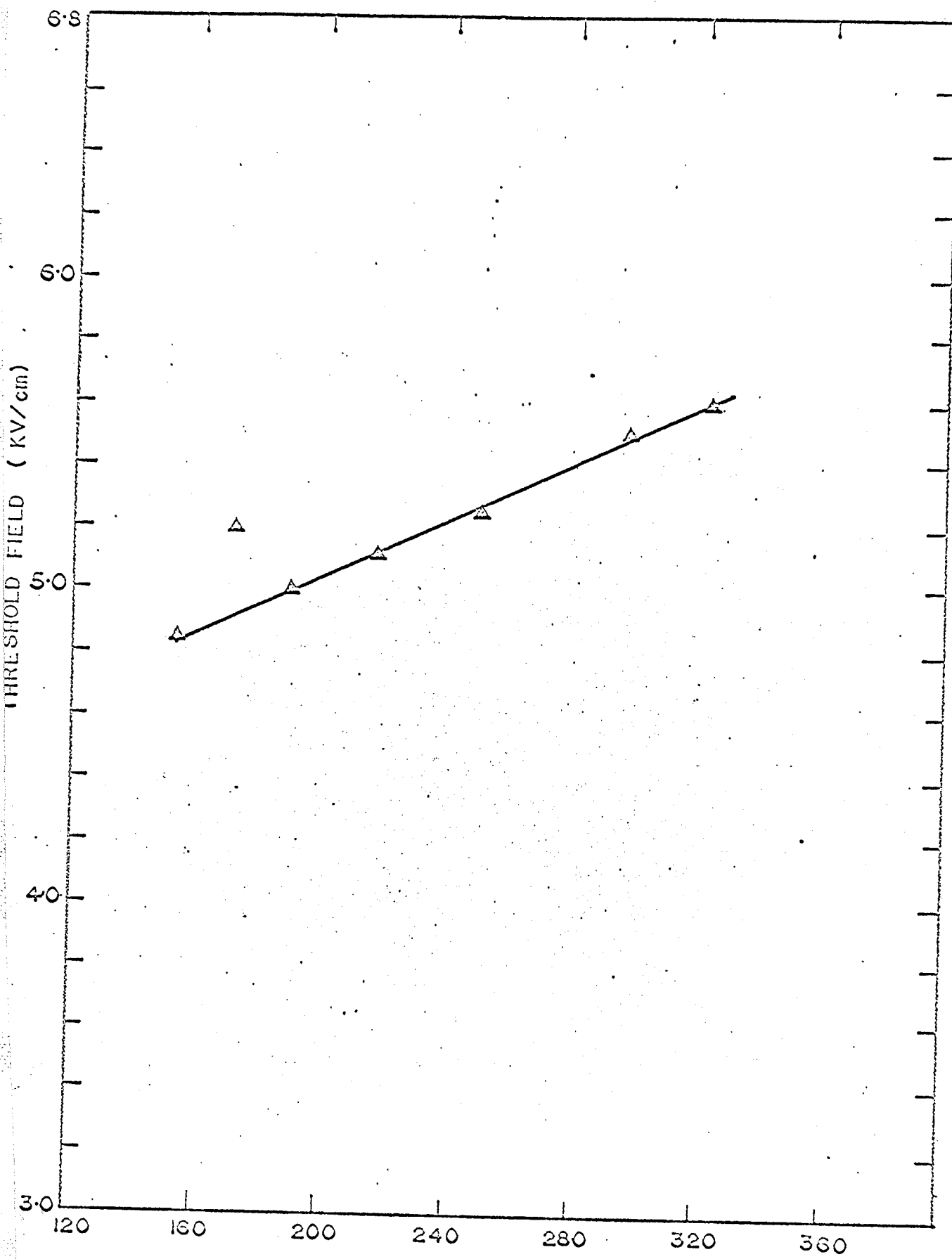


Fig.16. THE EFFECT OF TEMPERATURE ON THE THRESHOLD FIELD FOR CURRENT SATURATION.

mechanism (b).

(iv) It was also observed that the threshold field for the onset of current saturation decreases with increasing illumination intensity; and that the lower the temperature, the more pronounced is the saturation. This phenomenon can be explained by mechanism (b) as follows:  
The condition for the amplification of acoustic waves is given in Eqn. (4.1)

$$\mu_d E_{th} = V_s$$

Since (see Eqn. 2.4)

$$\mu_d = f_0 \mu_H$$

$f_0$  can be expressed as

$$f_0 = \frac{n}{n_t + n} \quad (4.2)$$

with increasing illumination the number of free carriers increases. Therefore,  $f_0$  increases with increasing illumination. The hall mobility  $\mu_H$  is given by:

$$\mu_H = R_H \sigma \quad (4.3)$$

where  $\sigma$  is the conductivity which increases with increasing illumination. From Eqn. (4.1) the threshold field  $E_c$  thus should decrease with increasing illumination for mechanism (b).

Fig. I7 shows that the photocurrent decreases and the threshold field increases with an increase in the doses of gamma-ray radiation in CdS films. This could be attributed to the increase in the number of traps due to radi-

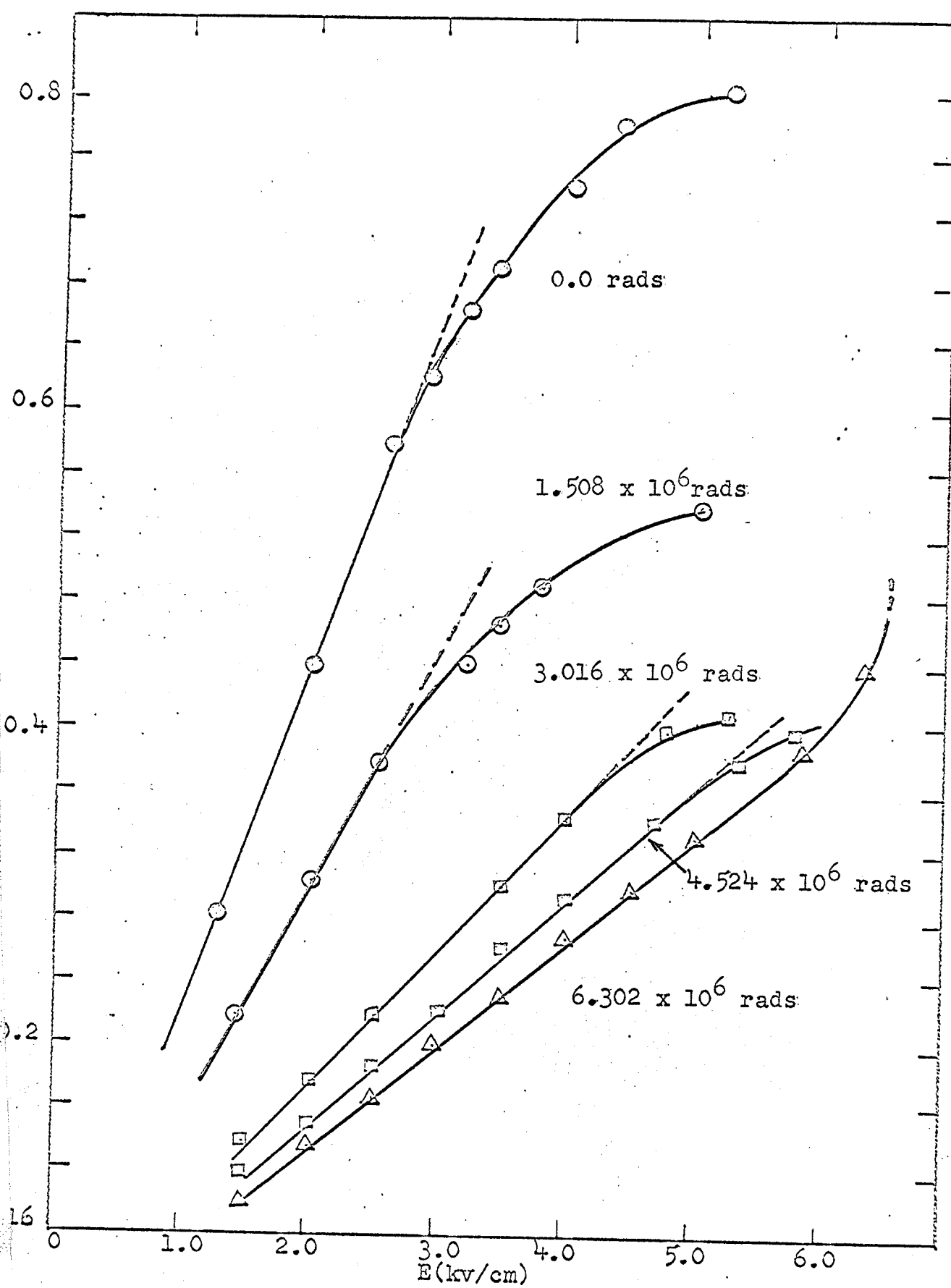


Fig.17 THE EFFECT OF GAMMA RAY RADIATION ON CURRENT SATURATION

ation. It increases the trapping factor  $f_0$  (see Eqn. 4.2) and hence decreases the mobility  $\mu_d$ . It could be seen from Eqn. (2.4) that with decrease in the mobility, it would require higher field for the onset of acoustoelectric current saturation and since:

$$I = n e N_d E \quad (4.4)$$

where  $n$  is the density of electrons;  $e$ , the charge of an electron;  $E$ , the applied field; and  $I$  is the photocurrent, therefore the photocurrent would decrease with decreasing mobility.

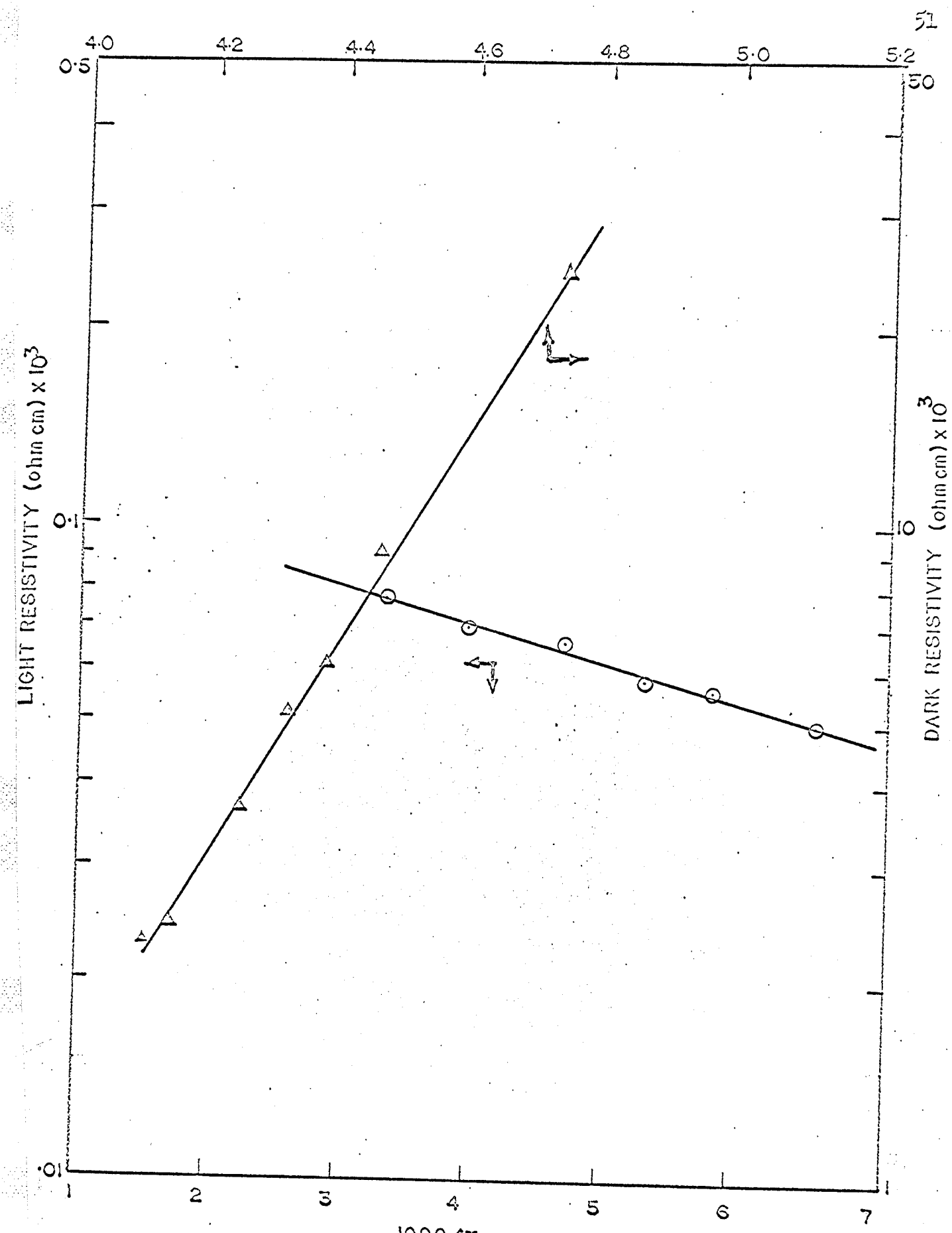


Fig. 18 THE DARK AND LIGHT RESISTIVITIES AS A FUNCTION OF  $1/T$

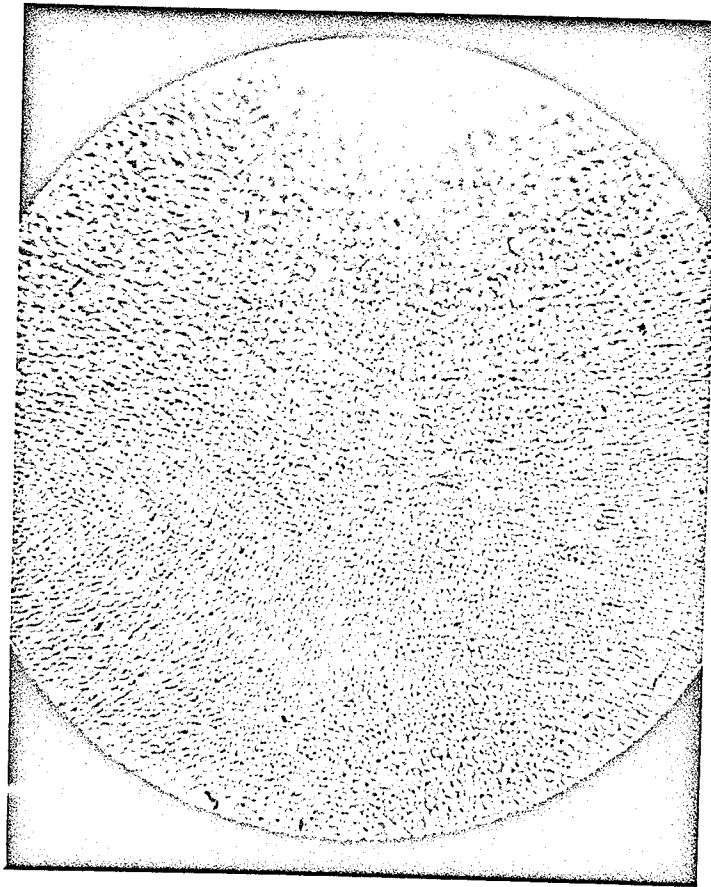


Fig. 19 PHOTOMICROGRAPH OF A VACUUM DEPOSITED CdS FILM  
(magnification  $10^3$ )

## CHAPTER 5

## CONCLUSION

When the velocity of electrons exceeds the velocity of sound, the coupling between phonons and electrons results in saturation or oscillation in bulk piezoelectric semiconductors. The inhomogeneity in crystals tends to enhance the acoustoelectric effect and this advantage has been used for the present study of this effect. The carrier mobility observed in films is considerably lower than that in crystals and this is attributed to the presence of native and foreign defects. Post-evaporation heat-treatment increases the mobility in films and recrystallizes the structure. On the basis of the analysis of the experimental results at various temperatures and illuminations, the current saturation in Cds films is attributed to acoustoelectric effect.

BIBLIOGRAPHY

- Albers, W., "Physical chemistry of defects", Physics and Chemistry of II-VI Compounds, North-Holland Publishing Co., pp. 167-222 (1967).
- Berger, H., "Elektronenmikroskopische untersuchungen an CdS-Und Cd-schichten", Phys. Stat. Solidi, 1, 679-84 (1961).
- Berger, H. et al, "Thickness dependence of conductivity due to polycrystalline structure in CdS thin films", Phys. Stat. Solidi, 28, K97-100 (1968).
- Boer, K.W., "Layer like field inhomogeneities in homogeneous semiconductors in the range of N-shaped negative differential conductivity", Physical Review, 139, A1949-A1959 (1965).
- Boer, K.W. et al, "Evaporated and recrystallized CdS layers", Jour. of Appl. Phys., 37, 2664-2677 (1965).
- Boyn, R. et al, "Incorporation of Cd-Interstitial double donors into CdS single crystals", Phys. Stat. Solidi, 12, No. 57, 57-70 (1965).
- Butler, M.B.N. and Sandbank, C.P., "Characteristics and applications of domains in semiconducting CdS," Trans. IEEE, ED-14, 663-668 (1967).
- DeKlerk, J. and Kelly, E.F., "Vapour-deposited thin-film piezoelectric transducers", Review of Scientific Instruments, 36, 506-510 (April, 1965).

- Dresner, J. and Shallcross, "Crystallinity and electronic properties of evaporated CdS films", *Jour. Appl. Phys.*, 34, 2390-95 (Aug. 1963).
- Faeth, P.A., *Journal of Electrochemical Society*, 114, 511 (1967).
- Foster, N.F., "Structure of CdS evaporated films in relation to their use as ultrasonic transducers", *Jour. of Appl. Phys.*, 38, 149-159 (Aug. 1966).
- Foster, N.F. et al, "Cadmium sulphide and Zinc Oxide thin film transducers", *IEEE Trans.*, SU-15, 28-41 (Jan. 1968).
- French, J.C., "A survey of second breakdown", *Trans. IEEE*, ED-13, 613 (1966).
- Froom, J., "An analysis of current instabilities in semi-insulating piezoelectric crystals", *Trans. IEEE*, ED-14, 656-659 (1967).
- Fukunishi, S. et al, "C-axis orientation of vacuum deposited CdS film", *Japan J. of Appl. Phys.*, 10, 1274-1275 (1969).
- Gilles and Van Cakenberghe, "Photoconductivity and crystal size in evaporated layers of cadmium sulphide", 182, 862-863 (1958).
- Greebe, C.A.A.J., "The influence of trapping on the acousto-electric effect in CdS", *Trans. IEEE*, SV-13, 54-64 (1966).
- Gurevich, V.L., "Theory of acoustic properties of piezoelec-

- tric semiconductors (Review)", Soviet Physics Semiconductors, 2, 1299-1325 (1969).
- Hamaguchi, C., "Effect of conductivity on current saturation in CdS", Japan J. Appl. Phys. 3, 491-492 (1964).
- Hamaguchi, C. et al, "Electron mobility in CdS determined from threshold field for current saturation, Japan J. Appl. Phys., 492-493 (1964).
- Haydl, W.H. and Quate, C.F., "High field domains in cadmium sulphide", Phys. Letters, 20, 463-464 (1966).
- Haydl, W.H. et al, "Current oscillations in piezoelectric semiconductors", 38, 4295-4309 (Oct. 1967).
- Hutson, A.R., "Piezoelectricity and Photosensitivity in ZnO and CdS", Phys. Rev. Letters, 4, 505 (1960).
- Hutson, A.R. et al, "Ultrasonic amplification in CdS", Phys. Rev. Letters, 7, 237 (1961).
- Hutson, A.R., "Acousto-electric explanation of non-ohmic behaviour in piezoelectric semiconductors and Bismuth", Phys. Rev. Letters, 9, 296-298 (1962).
- Jacob, J.E. and Hart, C.W., "Use of CdS layers in photo-cells", Proc. of National Electronics Conference, III, 1- (1955).
- Kikuchi, M., "Continuous oscillation in CdSe observed by local illumination", Jap. J. Appl. Phys., 2, 812-813 (1963).

- Kikuchi, M., "Experimental observations of undamped current oscillations in CdSe single crystals", Jap. J. Appl. Phys., 3, 448-458 (1964).
- Kikuchi, Y., "Temperature dependence of electron drift mobility for ultrasonic amplification in cadmium sulfide in relation to electron trapping effects", 6, 1251-1252 (1967).
- Kikuchi, Y. et al, "Temperature dependence of ultrasonic amplification in CdS", Trans. IEEE, SU-16, 189-200 (Oct. 1969).
- Kikuchi, Y., "Use of obliquely cut piezoelectric semiconductors of class (6mm) crystals for ultrasonic amplifiers", Trans. IEEE, SU-16, 200-206 (Oct. 1969).
- Kromer, H., "Proposed negative mass microwave amplifier", Phys. Rev., 109, 1556-1560 (1958).
- Lahiri, S.K., and Nag, B.R., "Build-up time of an acoustoelectric oscillator", Solid State Electronics, 12, 497-500 (1969).
- LeComber, P.G., "Transient acoustoelectric interaction in CdS and ZnS crystals", Brit. J. Appl. Phys., 17, 467 (1966).
- Lorenz, M.R., "Thermodynamics, materials preparation and crystal growth", Physics and Chemistry of II-VI Compounds, North-Holland Publishing Co., Chapt. 2, 73-115 (1967).
- Mason, I.M., "Acoustoelectric interactions in cadmium sulphide

- thin films", 1968 (Private communication).
- Moore, A.R. and Smith, R.W., "Effect of traps on acousto-electric current saturation in CdS", Phys. Rev., 138, A1250-A1258 (May, 1964).
- Moore, A.R., "Acoustoelectric current saturation in CdS as a fluctuation process", Jour. of Appl. Phys. 38, 2327-2339 (April, 1967).
- Neuclorfer, M.L., "Computer analysis of current instabilities in piezoelectric semiconductors", Trans. IEEE, ED-16, 1069-1076 (Dec. 1969).
- Nine, H.D., "Photosensitive attenuation in CdS", Phys. Review Letters, 4, 359 (1960).
- Okada, J., "Ultrasonic attenuation and some related behaviours in irradiated alkali halide crystals", J. Phys. Soc. of Japan, 18, 135-141 (1963).
- Paramenter, R.H., "Acoustoelectric effect", Phys. Rev., 113, 102-109 (1959).
- Prohofsky, "Acoustic waves in piezoelectric materials", J. Appl. Phys. 37, 4729-4738 (1966).
- Rose, A., "Acoustoelectric effects and the energy losses by hot electrons I", R.C.A. Review, 27, 98-139 (1966).
- Rose, A., "Acoustoelectric effects and the energy losses by hot electrons II", R.C.A. Review, 27, 600-631 (1966).
- Rose, A., "Acoustoelectric effects and the energy losses by hot electrons III", R.C.A. Review, 28, 634-652 (1967).
- Scott-Monck, A., "Barriers at evaporated metal-polycrystalline CdS interfaces", Appl. Phys. Letters, 9, 145 (1966).

- Smith, R.W., "Current saturation in piezoelectric semiconductors", Phys. Rev. Letters, 9, 87 (1962).
- Somorjai, G.A., "Effect of light on the evaporation and oxidation of CdS single crystals", Surface Science, 2, 298 (1964).
- Stanley, I.W., "Damping of sustained current oscillations in semiconducting cadmium sulphide at high fields", Appl. Phys. Letters, 10, 76-78 (1967).
- Uchida, I. and Ishiguro, T., "Excited current noise in non-ohmic region of CdS," Jour. Phys. Soc. of Japan, 24, 661-662 (1968).
- Uchida, I., "Current noise induced by electron phonon interaction in semiconducting CdS crystals", Japan J. Appl. Phys., 1295-1296 (1968).
- Uchida, I., "Round trip oscillation in the first current saturation of CdS crystals", Jap. J. Appl. Phys., 8, 119 (1969).
- Wang, W.G., "Strong acoustoelectric effect in CdS", Phys. Rev. Letters, 9, 443 (1962).
- White, D.L., "Amplification of ultrasonic waves in piezoelectric semiconductors", Jour. Appl. Phys., 33, 2547-2553 (Aug. 1962).
- Woodbury, H.H., "Diffusion of Ag in CdS", Jnl. of Appl. Phys., 36, 2287 (1965).
- Woodbury, H.H., "Stoichiometric effects of O<sub>2</sub> on CdS", Jnl. Phys. and Chem. of Solids, 27, 1257 (1966).

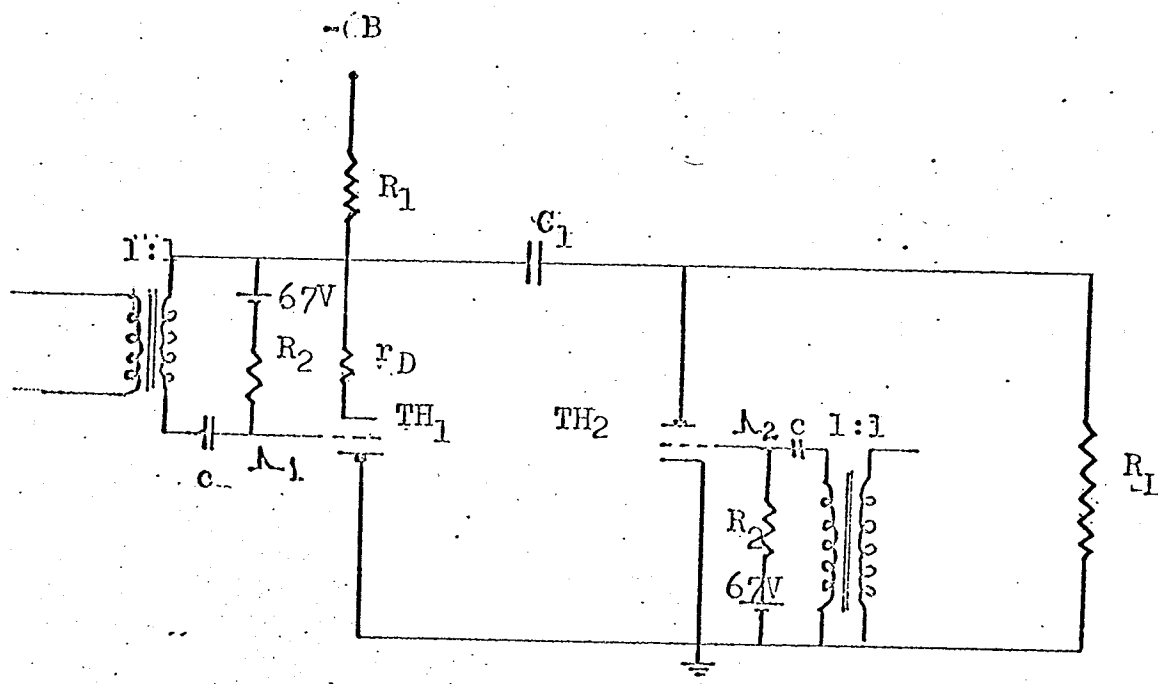
- Woodbury, H.H., "Diffusion and solubility studies", Physics and Chemistry of II-VI Compounds, Chapt. 5, North-Holland Publishing Co., 223-263 (1967).
- Yamamoto, R., "Current oscillations in CdS", Japan Jour. of Appl. Phys., 5, 351-357 (May, 1966).
- Yee, S. et al, "Current saturation and oscillation in CdSe", Solid State Electrons, 12, 191-199 (1969).

## APPENDIX

## DESIGN OF PULSE GENERATOR

A pulse generator was designed and built for the present investigation of V-I characteristics of CdS films. There were constraints on the pulse width and the shape of the pulse which could be satisfied only by using the circuit shown in Fig. 20. The pulse width had to be more than  $5\mu\text{sec}$  and variable, the pulse rise time and fall times had to be within a few microseconds and the top of the pulse was to be fairly smooth.

The design had two hydrogen thyratrons in parallel with the maximum plate ratings of 9.0 kV and 125 ampers. The capacitor  $C_1$  is first charged to the supply voltage through the resistance  $R_1$ , then thyratron 1 is fired by the trigger pulse 1 and the supply voltage appears across the load resistor  $R_L$ . After a desired amount of delay, which could be controlled by the trigger generator, thyratron 2 fired and put a short circuit across the load resistor. Thus, by a simple on-off sequence of the thyratrons, rectangular pulses of a desired width (from  $5\mu\text{sec}$  to  $150\mu\text{sec}$ ) could be generated. By using a damping resistor  $R_D$  the top of the pulse was made fairly smooth. The rise and decay times of the pulse were found to be of the order of  $2-3\mu\text{sec}$ . The wave shapes of output pulses are shown in Fig. 21 A&B.



$$R_1 = 500 \text{ K ohm}$$

$$C_1 = 1.0 \mu\text{F}$$

$$r_D = 10 \text{ ohm}$$

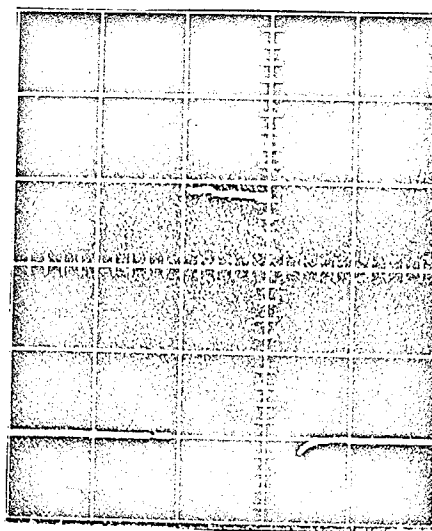
$$C_2 = 0.1 \mu\text{F}$$

$$R_2 = 3 \text{ K ohm}$$

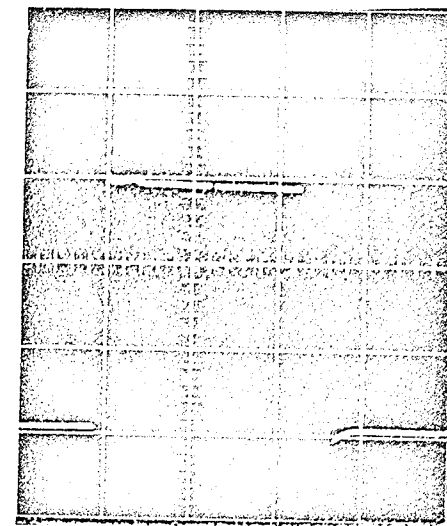
$$B = 0-6 \text{ kv.}$$

$$R_L = 1 \text{ K ohm}$$

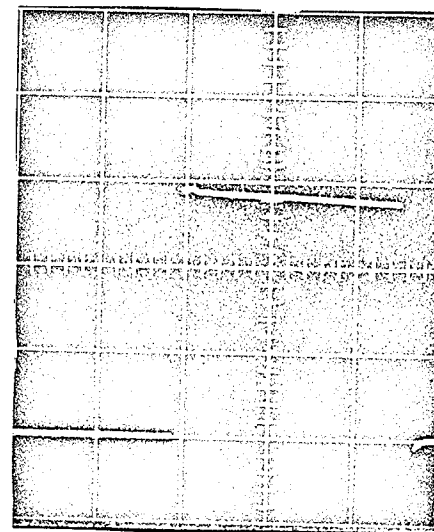
Fig. 20 CIRCUIT DIAGRAM OF THE PULSE GENERATOR



600 Volts 10  $\mu$ secs

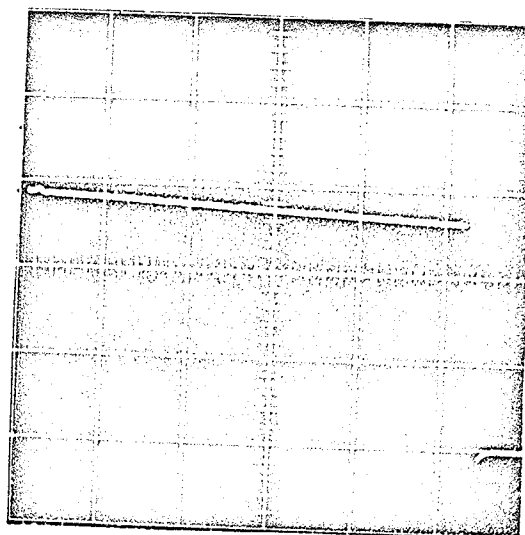


600 Volts  $\mu$ 22 secs

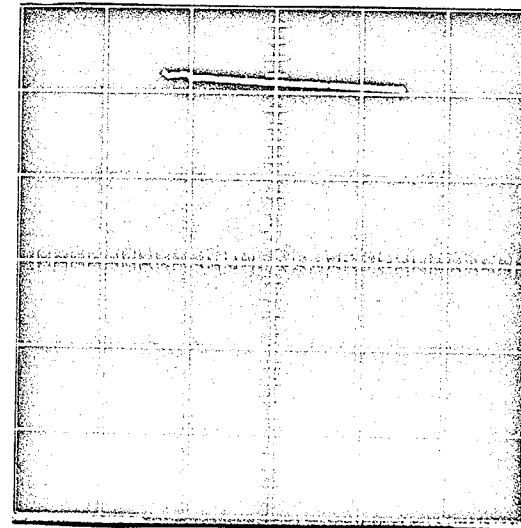


600 Volts 50  $\mu$ sec.

Fig. 21 A OSCILLOSCOPE PHOTOGRAPHS OF THE OUTPUT PULSES OF THE GENERATOR.



600 Volts      100 $\mu$  secs.



1.0 kv      30 $\mu$  secs.

Fig. 21 B OSCILLOSCOPE PHOTOGRAPHS OF THE OUTPUT  
PULSES OF THE GENERATOR